POLITECNICO DI TORINO

Facoltà di Ingegneria

Corso di Laurea Magistrale in Ingegneria Biomedica

Master Thesis

Effect of the Electrical Stimulation Site on Architectural Changes in Tibialis Anterior

Implications for the reduction of fatigue during electrically-induced contraction

Advisors:
Prof. Alberto Botter
Prof. Marco Gazzoni

Candidate:
Marco Carbonaro

Anno Accademico 2018/2019

To my mother, my father and my brothers

Because limits, like fears, are often just an illusion.

Michael Jordan

Acknowledgements

I thank my advisor Prof. Alberto Botter and all Lisin members for giving me the opportunity and the means to work in this context and for all their help.

First of all, I would like to thank my Mother and my Father to have made all of this possible and for supporting me throughout everything.

I'm especially grateful to my two brothers, Andrea, and Matteo for showing me how to build myself since I was a kid.

I would also like to thank Giulia for becoming part of the family and for allowing me to play with my nephew Alessandro since he came into our lives.

I want to thank also all my "biofriends", especially Davide that follow exactly my route since the first day of the first university year.

Thanks to my best Friend, the Basketball, to always be my lifeline and for giving me so many teammates and friends.

Last but not least, thanks to my Love Clelia for choosing me to live this and all future adventures.

Summary

Electrical Stimulation of skeletal muscles is commonly adopted in both research and clinical settings with the purposes of preserving or recovering muscle mass (rehabilitation), improving muscle function (training) and restoring purposeful movement after CNS damage (neuroprosthesis). When the stimulation is used to accomplish functional movements and actions, it is referred to as the Functional Electrical Stimulation (FES).

Electrically-induced muscle contractions can be obtained by delivering electrical pulses over a peripheral nerve trunk (nStim) or to the terminal nerve branches at the muscle level (mStim, referred to as NMES). Noteworthy, muscle contractions generated by electrical stimulations are associated with rapid development of neuromuscular fatigue. To reduce the issue of fatigability in electrically-elicited contractions, several types of stimulation have been developed. Different approaches were sought to to reduce the overall Motor Unit (MU) discharge rates and increase spatial MU recruitment (e.g. distributed and sequential stimulation), but also to achieve a more physiological MU recruitment order relying on reflex pathways (e.g. afferent stimulation).

Among the methods for fatigue reduction, Interleaved stimulation (iStim) is a recent approach in which electrical stimuli are intermittently provided to muscle and nerve sites to stimulate different populations of MU. The extent to which fatigue is reduced with iStim depends on the degree of overlap between the populations of MUs activated by the two stimulations (i.e. mStim and nStim). In general, groups of MUs activated by either mStim or nStim are different because of the different MU recruitment order of nStim and mStim (i.e. inverse vs random). Geometric factors may

also play a relevant role in this differentiation, indeed superficial MUs (those closest to the stimulating electrodes) are recruited preferentially during stimulation over a muscle belly (mStim), whereas for stimulation over the CP nerve trunk (nStim), it was found that recruited MUs were randomly distributed evenly throughout the muscle regardless of stimulation amplitude.

In this study we investigated whether and to which degree the stimulation site (mStim or nStim) affected the architectural changes in the superficial and deep Tibialis Anterior (TA) compartments. For this reason, Ultrasound (US) imaging was used to quantify muscle tissue displacement associated with MU activations by measuring morphometric parameters, such as Muscle Thickness (MT), Fascicle Length (FL) and Pennation Angle (PA) during contractions evoked by nStim, mStim and voluntarily performed. It was found that architectural changes in nStim contractions were similar to those observed in voluntary contraction (i.e. the PA and FL of the superficial and deep muscle portions changed similarly). Instead, mStim contractions led to a relevant activation (and architectural changes) of the upper compartment compared with the deeper one. These findings suggest that in TA interleaved stimulation can be used to activate different muscle portions, with possible implications for the reducion of electrically-induced fatigue. Indeed, by interleaving the recruitment of different MUs either located superficially (during mStim) or distributed throughout the muscle (during nStim), this type of stimulation allows to obtain the required force output with a low-frequency activation of different MU populations.

The potentialities of iStim in reducing muscle fatigue was tested in a proof-of-concept experiment where the mechanical manifestations of fatigue induced by mStim, nStim and iStim were compared in one subject. Strikingly, iStim doubled the "time to task failure" of both mStim and nStim, confirming the hypothesized potentialities of this stimulation approach.

Table of Contents

List of Figures

List of Tables

List of Acronyms

NMES	Neuromuscular electrical stimulation
MN	Motor Neuron
SCI	Spinal Cord Injury
CNS	Central Nervous System
FES	Functional electrical stimulation
EMG	Electromyography
AP	Action Potential
CMAP	Compound muscle action potential
MU	Motor Unit
MP	Motor Point
mStim	muscle stimulation
nStim	nerve stimulation
TA	Tibialis Anterior
FL	Fascicle Length
PA	Pennation Angle
MT	Muscle Thickness

LPR	Low Pulse Rate
WPHF	Wide-pulse High-frequency
Vol	voluntary contraction
US	ultrasound
CP	Common Peroneal
PL	Peroneus Longus
MVC	Maximum Voluntary Contraction
ROI	Region of Interest
iStim	Interleaved stimulation

Chapter 1

Introduction

1.1 Electrical stimulation of the peripheral nervous system

1.1.1 Introduction

Electrical stimulation of the peripheral nervous system involves the application of sequences of stimuli intermittently to superficial skeletal muscles, applied over intramuscular axonal branches, that is commonly named as NMES, or over Motor Neuron (MN) axons (called nerve stimulation), with the main purpose of triggering visible muscle contractions [1]. Artificially elicit muscle contractions and produce limb movements is often perceived as something strange and wonderful [2]. In the last past years, NMES increased its popularity, given the possibilities it offers for a number of research and clinical applications [3], and other many fields of interest. For example: in normal subjects and athletes, NMES is used to generate contractions for training [4], [5]; in patients following stroke, Spinal Cord Injury (SCI) or damage to the Central Nervous System (CNS) which are unable to perform volitional exercise, it is used as rehabilitation tool (to maintain muscle function during a phase of limited activity) [6]; but it can also restore purposeful movements [7].

1.1.2 Functional electrical stimulation (FES)

Thus the acronym FES is probably the most commonly used in literature [8]. FES started as a process of combining simultaneous or intermittent stimulation with a functional task [9] and became therefore a method to trigger artificially the sensory motor system inducing activations in paralysed or weakened muscles in particular after an injury/disease of the CNS that attempted to alleviate the resulting disability [10]. In fact, it can be used to bypass the disconnected pathways between the CNS, and lower extremity muscles. The basic requirements are technology for actuators (for selective muscle activation) and sensors (for feedback) with conditioning circuit and a control system to pilot the stimulator [11]. FES has two main application relative to the time period in which this type of tool is implemented: without temporal limits (because it allows the patient to perform functions that otherwise would not be possible), or in limited period (in order to stimulate motor learning useful for performing a function). However, a classification may be made on the basis of intent:

- *FES Neuroprosthesis:* implemented permanently with the goal of recreating a movement as close as possible to the physiological one. One of the first clinical trials that used electrical stimulation for muscle function, was a device that stimulates the peroneal nerve in the leg in an attempt to correct drop foot in people with hemiplegia, associated with stroke, during ambulation (Fig. 1.1 A) [12]. Another common application is in Hand Grasping, stimulating selectively muscles of the hand and forearm to open the hand, close the hand and maintain grabbed an object in the hand (Fig. 1.1 B).

- *FES Training:* used in order to induce a neuromuscular and cardiovascular conditioning aimed at improving the general physical condition of the subject. In this case the goal is to maximize the training intensity (fatigue) with high compliance (e.g. pleasant and comfortable activities). In this situation, the oxygen consumption is maximal due to hybrid contraction (i.e. integrating voluntary and electrically-induced contraction). For instance, in paraplegia training is quite important to avoid issues such as infection, obesity, type II diabetes and

coronary heart disease [13], [14]. Some examples are: FES cycling and the innovative FES rowing (Fig. 1.1 C and D). The controlling system in such a case can be open-loop (i.e. the subject may control the stimulation properly) either close-loop (i.e. the subject is not required to manage the stimulation).

- *FES Therapy:* used for a limited period of time to stimulate the motor learning (i.e. rehabilitation tool). It is indeed based on mechanisms of neuroplasticity that allow to promote the re-learning of motor functions. In this case the aim is to involve the subject in compliant and relevant activity.

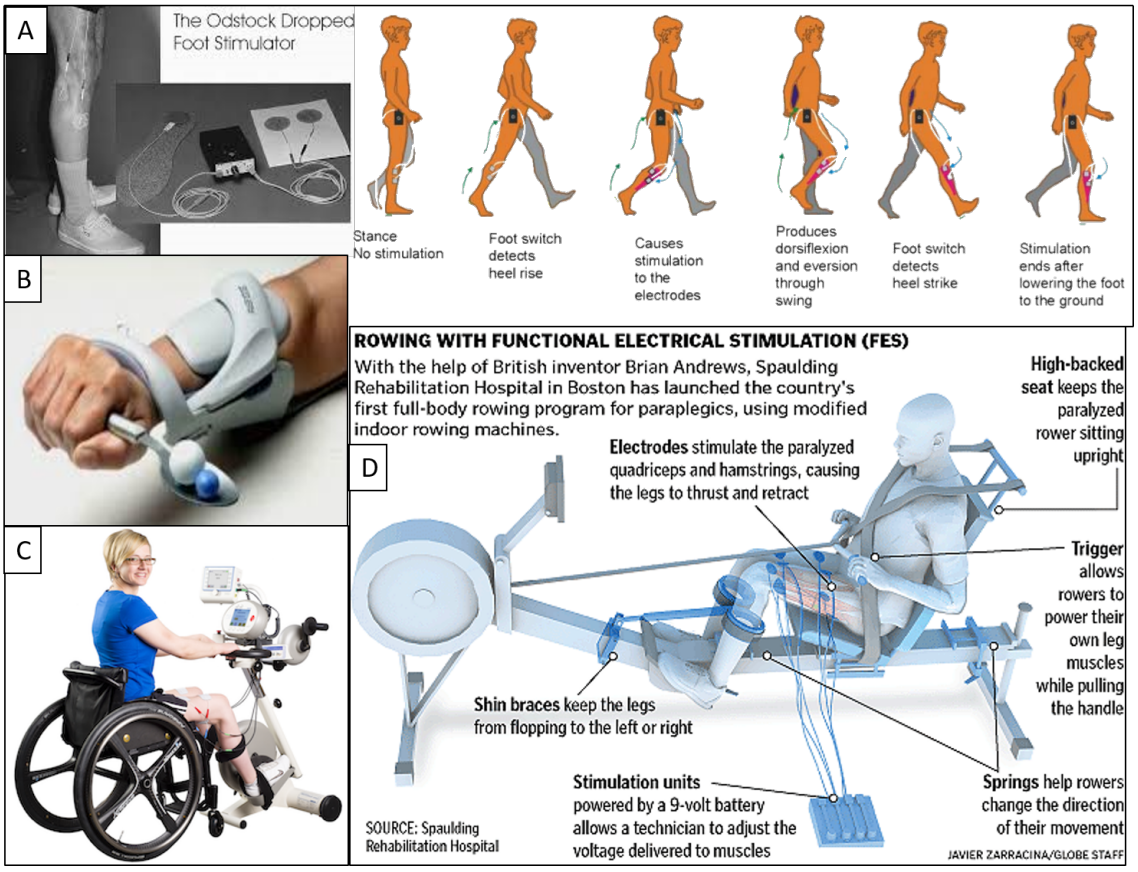

Figure 1.1: Examples of Functional electrical stimulation (FES): Odstock dropped foot stimulator and its functioning (A), Handmaster NESS H200 (B), RehaMove FES Cycling (C), FES rowing (D).

1.1.3 Stimulation techniques

Electrical stimulation of the peripheral nervous system involves different neural structures. In general, an electrical field is generated by application of bursts of short current pulses. A region of depolarization is usually triggered by this kind of stimulus on the target (i.e. nerve trunk or terminal branches, Fig. 1.2) due to activation of ions channels (the transmembrane voltage threshold is exceeded) and consequent induction of ionic currents that generate a self propagating Action Potential (AP) [15]. The electrical field can be generated by electrodes placed near nerves (nerve stimulation) or above a muscle motor point (motor point stimulation) with two common techniques: monopolar or bipolar configuration (Fig. 1.2) [16].

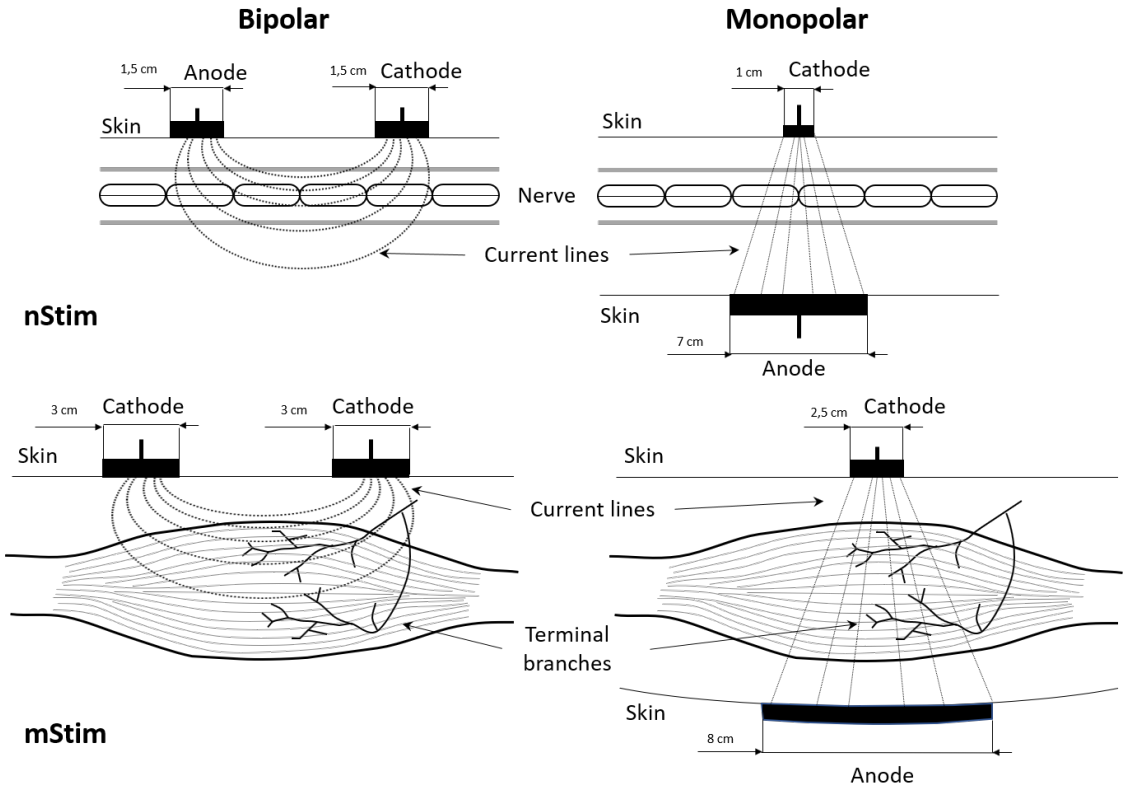

Figure 1.2: Schematic representation of bipolar and monopolar electrode configuration applied over nerve (nerve stimulation (nStim)) and muscle (muscle stimulation (mStim)), with example of electrode size

In the monopolar arrangement, the stimulation effect only one of the two stimulation electrodes and in particular the smallest one (few square centimetres) whereas the second larger electrode is generally placed contralateral over the antagonist muscle (often for large muscle stimulation) or usually above bony protrusions (e.g patella or elbow, etc..) for both nerve and muscle stimulation. In case of bipolar configuration, the size of the two electrodes is similar and depends on which structure (i.e nerve or muscle stimulation) you want to elicit. Obviously the position of electrodes is a critical issue: for mStim, a precise localization of muscle MPs is of primary importance (i.e. location where the motor branches of a nerve enter the muscle belly), and hence atlas of MP positions support this trouble [17]; rather then for nStim an appropriate knowledge of the anatomy of the muscle and the related innervations in which you want to induce a contraction is necessary (e.g. Netter [18]). Moreover, proper identification of MP or innervation zone (that do not necessarily coincide but are often close to each other), optimize the stimulation paradigm, avoiding also the use of uncomfortable current levels with the main aim to maximize the output force.

1.1.4 Neural pathways: M-waves and H-reflex

It is important to note that every nerve innervating a muscle contains motor efferents to the muscle (efferent neural pathways) and multiple sensory or afferent nerves (afferent neural pathways), as it is possible to see in the model in Fig. 1.3 A. Triggering an efferent pathways cause the direct activation of muscles that are innervated by neurons. In general, when the nerve is excited in a way that produce a muscle twitch, it is possible to record via Electromyography (EMG) an M-wave [also termed Compound muscle action potential (CMAP)] [19] (see Fig. 1.3 B). In parallel, various reflexes are generated due to arrival of APs to the spinal cord that trigger activity in afferent pathways. In this case, if a muscle twitch is induced, an H-reflex (Hoffmann reflex) is recorded [20], [21] (see Fig. 1.3 C). The H-reflexes are produces by Ia afferents (because have a lower electrical threshold than αMNs) specially due to stimuli of relatively long duration [22].

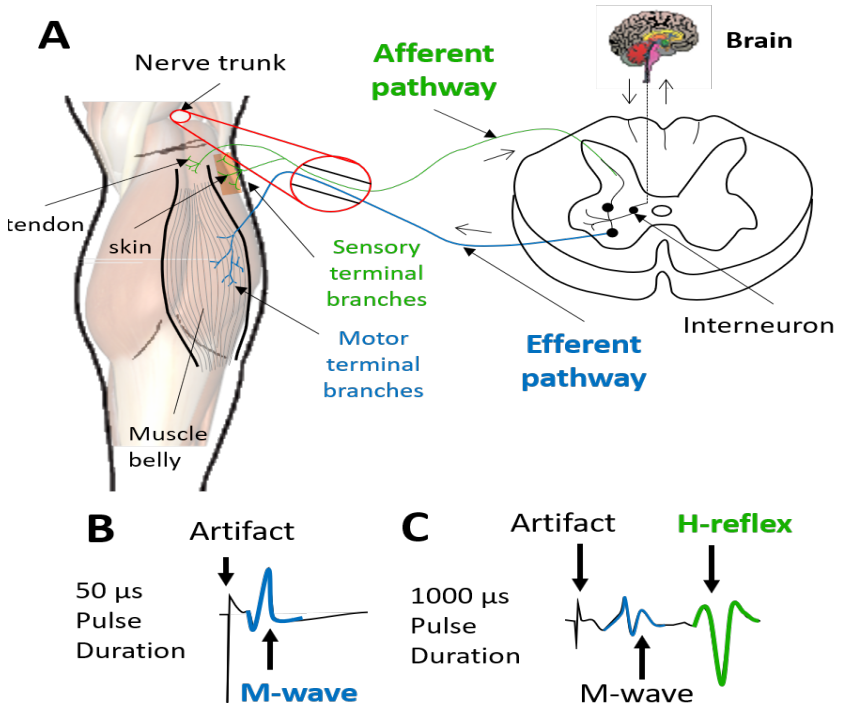

Figure 1.3: (A) Model of the effects of peripheral electrical stimulation. A sample of M-waves (B) and H-reflex (C) generated by a single rectangular pulse of different duration [23]

When the stimulation intensity is progressively increased several corresponding volleys in Ia afferents and motor axons are generated (Fig. 1.4). When the current intensity is low (e.g. 9 mA) Ia afferents will be only elicited that activate MNs which fire in the H-reflexes (Fig. 1.4 (a), (e)). With stronger stimulation (e.g. 12 mA) more Ia afferents would be activated that causes higher number of MNs to fire in the H-reflex (i.e. the traces increase in amplitude Fig. 1.4 (b), (f)). In this case, an axon motor volley appears and finally an M-wave arise in the EMG too. Reflex responses of MN would collide with antidromic motor volleys (i.e. in opposite direction referred to the muscle). Even stronger stimulation (e.g. 15 mA) leads MNs to fire in the H-reflex, but also more motor volleys will be elicited in the axons; as a result, more M-waves appear in the muscle fibers (Fig. 1.4 (c), (d)). In this situation, antidromic motor volleys collide with and eliminate reflex volleys in the axons, generating a reduction of H-reflex size. Yet stronger stimulation (e.g. 30 mA)

leads to produce maximal M-wave and for the most part H-reflexs are eliminated by the antidromic collision (Fig. 1.4 (d), (h)).

For all these reasons, the CNS is multimodally "bombarded" by NMES [7], and the results involves spinal motor neuron facilitation [24] and increased cortical activity and cortico-spinal excitability. It has been finally demonstrated an "acute" involvement of spinal motor neurons which occurs during NMES, a phenomenon that is based on a reflexive MN recruitment; it is also responsible for involuntary muscle phenomena that persist after the end of stimulation (e.g muscle cramps) [25].

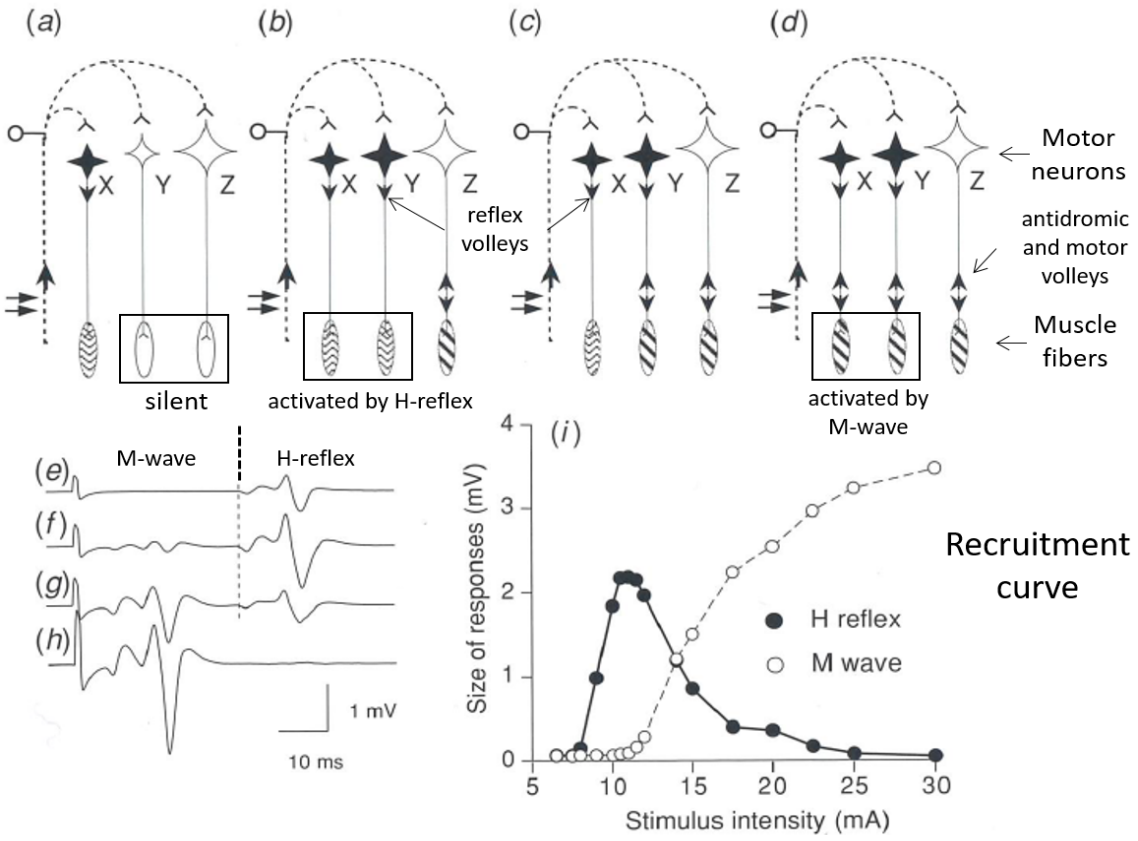

Figure 1.4: Example of recruitment curve of the H and M waves in a muscle. Sketches of the volleys in Ia afferents and motor axons ((a)-(d)) when the stimulus intensity is progressively increased, and the corresponding EMG responses ((e)-(h)). The recruitment curve represents the amplitudes of the H-reflex and the M-waves plotted against stimulus intensity. [22]

1.1.5 MU recruitment in electrically-induced and voluntary contraction

Any muscular activation triggered from external differs from activation by a voluntary motor command by an upper MN [26]. In case of voluntary contraction, the number of activated MNs and their discharge frequency are controlled by the CNS, hence registering EMG every contributes of a MN are asynchronously summed, generating a random signal (stochastic) , also named as myoelectric interference signal (Fig. 1.5 A). In case of electrically-induced contraction, CNS loses all control role over muscle, and the MUs are recruited synchronously with the stimulation frequency and the number of MUs are related to the current intensity (Fig. 1.5 B).

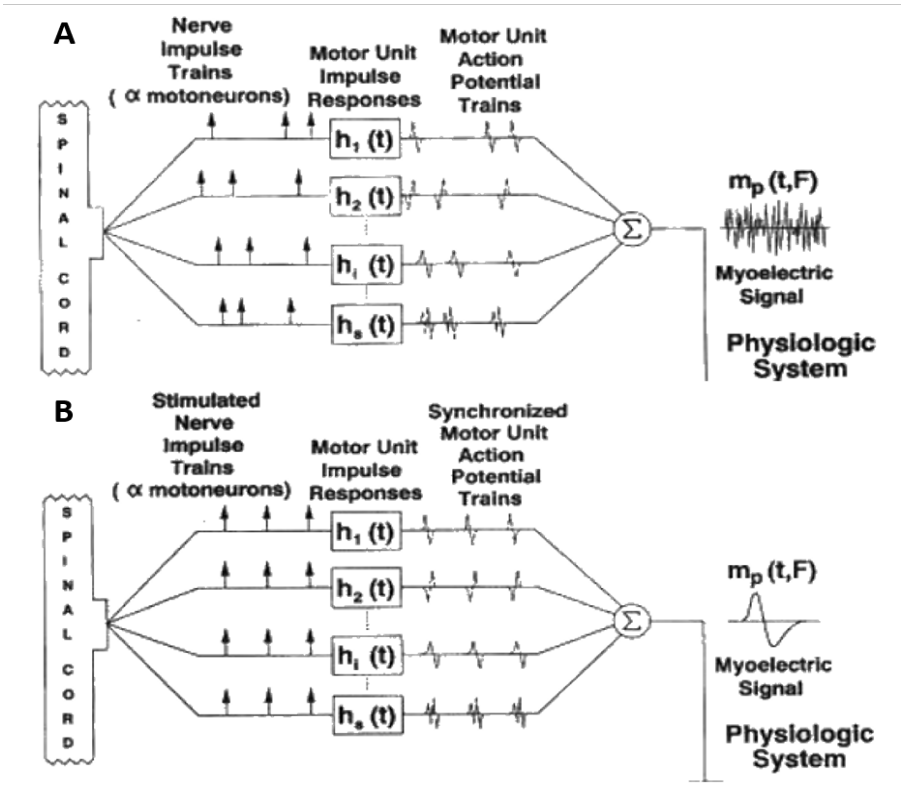

Figure 1.5: Schematic representation of the mode of generation of the cutaneous myoelectric signal during voluntary (A) and electrically-induced (B) contractions [27].

Certainly one of the main limitations regarding any non-physiologically induced muscle activation, concern the strong discomfort related to the current dose, associated with the peripheral stimulation [28], that is stronger in case of NMES and a bit lower for stimulation released over nerve trunks. Other two main significant limitations are: the overall decreased efficiency of contraction (i.e the output force produced) and the propensity for development of neuromuscular fatigue [29]. In particular the differences are related with the MUs recruited (see table 1.1) during the contraction in terms of spatial recruitment that is imposed to the same muscle fiber pool (i.e., in case of muscle stimulation, those superficial with the motor terminal branches close to the electrode stimulants, and in case of nerve stimulation, those probably more dispersed that are innervated by the stimulated axon), instead of more dispersed along the whole muscle belly such as during voluntary contraction. In both stimulation site (nerve or muscle), new fibers could be depolarized if current intensity is progressively increased, therefore fibers more distant from the electrode (i.e., deeper) during muscle stimulation [30], while contractile activity is maintained by the superficial fibers; in nerve stimulation also other fibers innervated from the same trunk could be activated but this is more complicated because a trunk contains sundry nerves of different muscle. The next difference is quite logical, because the temporal recruitment, during electrically-induced contractions, is imposed by the stimulator synchronously (Fig. 1.5) [31]. Finally, the main argument supporting differences in MU recruitment is the order in terms of type of fiber (i.e type I small, slow and fatigue resistant and type II large, fast and more fatiguing) [32]. However, contradictory findings on motor unit recruitment order was studied by researchers. In fact, voluntary contraction follow the Hennemann's size principle [33]; on the other hand, the traditional view is that axons with greater diameter, which have a lower stimulation threshold than smaller, are more likely to be excited by imposed electric fields [34]. Indeed, some other researcher found minimal or no difference between voluntary and electrically elicited contractions [35]. Furthermore, it is supported the hypothesis that MU activation is non selective without obvious sequencing related to fiber features [36], [37].

	Voluntary	**Electrically-induced**
Spatial		
	Dispersed and quasi-complete	Superficial(mStim), dispersed (nStim) but fixed and largely incomplete
Temporal		
	Asynchronous	Synchronous
Order		
	Hennemann's size principle	Nonselective, random, disorderly

Table 1.1: Summary comparison between voluntary and electrically-induced contraction for what concern the MU recruitment [7].

However, the size of MN axon is not the only factor in recruitment order. Other factors are:

- Stimulation parameters (changes axonal excitability)

  Frequency

  Amplitude (current intensity)

  Pulse width;

- Electrodes

  surface area (size)

  placement (distance from axonal branches or trunks);

- Distribution and orientation of MUs;

- Contraction conditions (isometric, isotonic, dynamic);

- Muscle length and joint angle that vary the position of muscle fiber.

1.2 Methods to reduce fatigue in electrically-induced contractions

In literature there are 3 main methods that manipulate the above mentioned factors that influence the stimulation in fatigue enhancement, with main aim to reduce it:

- *Distributed stimulation*,
- *Afferent stimulation*,
- *Interleaved stimulation*.

1.2.1 Distributed stimulation

One first way to overcome the limitation of restricted number of superficial fiber recruited during NMES over a skeletal muscle, is to use more electrodes to stimulate different part of the muscle and hence obtain the activation of entire array of motor axons supplying that muscle [38]–[42]. Therefore, with relatively low stimulation rates (LPR protocol) of electrical stimulation delivered through multiple electrode locations on a single site, it is possible to produce a fused contraction. In addition to the distribution of electrode pads, the idea is to reduce the stimulation frequency on a single electrode and make it asynchronous between each pad (Fig. 1.6). Stimulation protocols involves sequential rotation of pulses between multiple active electrodes [43] that usually are spaced among them (in comparison to conventional single pad stimulation), or that are close together at the same site and over the same area (as the single electrode conventional stimulation) [44]. A further evolution is to randomize the pulses among multi-pad electrodes instead of having it in a sequential pattern [45]. Thus many studies evaluate reduction and delay of muscle fatigue without decreasing the output force (i.e. joint torque), with main benefits of activation of greater number of MU, reduced frequency. Usually this is evaluate on large muscle like knee extensors (i.e. quadriceps) and knee flexors that is an important drawback. Other two main limitations are the excessive discomfort associated with NMES and the fact that deep MUs are still not stimulated also because MU recruitment overlap between active electrodes raises, increasing stimulation intensity.

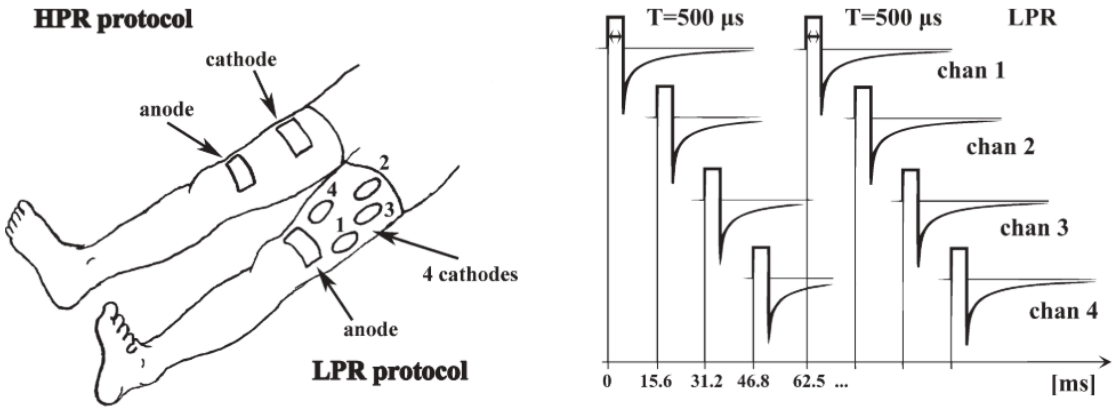

Figure 1.6: On the left: example of electrode placement for two protocols. Four electrodes used to deliver current pulses with the LPR protocol (showed on the right chart) from several channels (labeled 1–4). Stimulation was asynchronously delivered through four channels to the muscle, with the pulses equally ordered in time. [38]

1.2.2 Afferent stimulation

As already mentioned in paragraph 1.1.4, several reflex responses are generated by electrical stimulating field that activates afferent neurons [26]. To obtain this kind of reflexes (i.e. Hoffmann reflex, H-reflex), it is necessary to independently stimulate afferent fibers at a constant stimulation current that is below the motor axon rheobase current. As shown in Fig. 1.7 the rheobase current of the axons of type Ia (i.e afferent fibers) is typically lower than those of motor axons [46]. H-reflexes can be elicited at low currents level where one stimulus is insufficient, by multiple stimuli at high frequency (e.g. 100 Hz) [47], because of temporal summation of the Ia excitatory postsynaptic potential (EPSP) in the MNs [48]. As for the motor responses, this issue is strictly related to the electrode positioning [21]. Compared with conventional stimulation that has about 50-200 μs pulse width and 25-40 Hz frequency, eliciting reflexes needs wider pulses (i.e. up to 1 ms) and higher frequency (i.e. up to 100 Hz); for this reason this type of stimulation is also known as WPHF stimulation [49], [50]. Spinal MNs (i.e. large diameter afferents) would be recruited by sensory volley evoked by the wide pulses (1 ms).

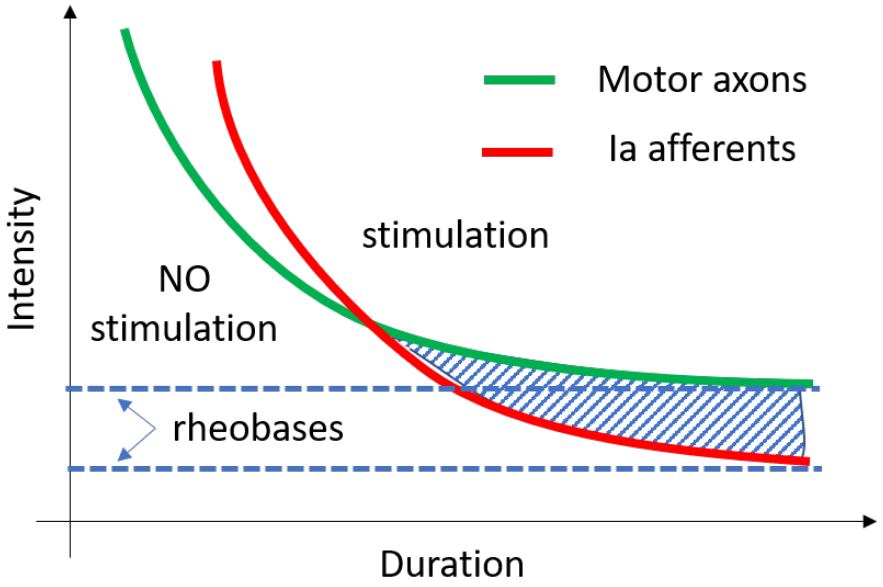

Figure 1.7: Intensity-Duration curve: correlates the intensity and duration of the stimulation so that the excitation of the membrane and the triggering of the AP occur. Stimulating the nerve with pulses with duration-intensity in the dashed area, it is possible to induce reflex responses.

In addition, the intensity of stimulation is much lower at the same force production and a lower number of peripheral motor axons (recruited randomly) will be depolarized. Reflected activation of MUs on the basis of the size principle leads to a more physiological recruitment order (greater proportion of type I MU). [51], [52]. Not every muscles has the possibility to be selectively activated from a nerve and also it can be difficult to evoke H-reflex in some of those muscles (e.g. TA). Thus, the main analysed muscles are the plantar flexors, i.e. soleus and gastrocnemii (medial and lateral). Another considerable drawback concerns the lower level of muscle activation together with a complicated control due to variability inter and intra subject.

As already mentioned (paragraph 1.1.4) an "acute" involvement of spinal motor neurons (based on reflexive MN recruitment) could generate a phenomenon referred to as *"central torque"* (Fig. 1.8). During a prolonged section of conventional NMES, an output torque increases first and then decreases progressively and this development of fatigue manifests itself in a "slowdown" of the EMG signals. A gradual decrease in the conduction velocity of the muscle fibre is the manifestation of this "slowdown" which occurs in a progressive enlargement of the M-wave. On the other hand, during the WPHF NMES, the torque, in addition to not decrease during the course of stimulation, increases significantly compared to that caused by conventional one (Fig. 1.8). This "extra" force might be caused by sensory volleys that could trigger either bistable or self-sustaining discharge of MNs, coherent with the occurrence of persistent inward currents in spinal MNs and interneurons. [25].

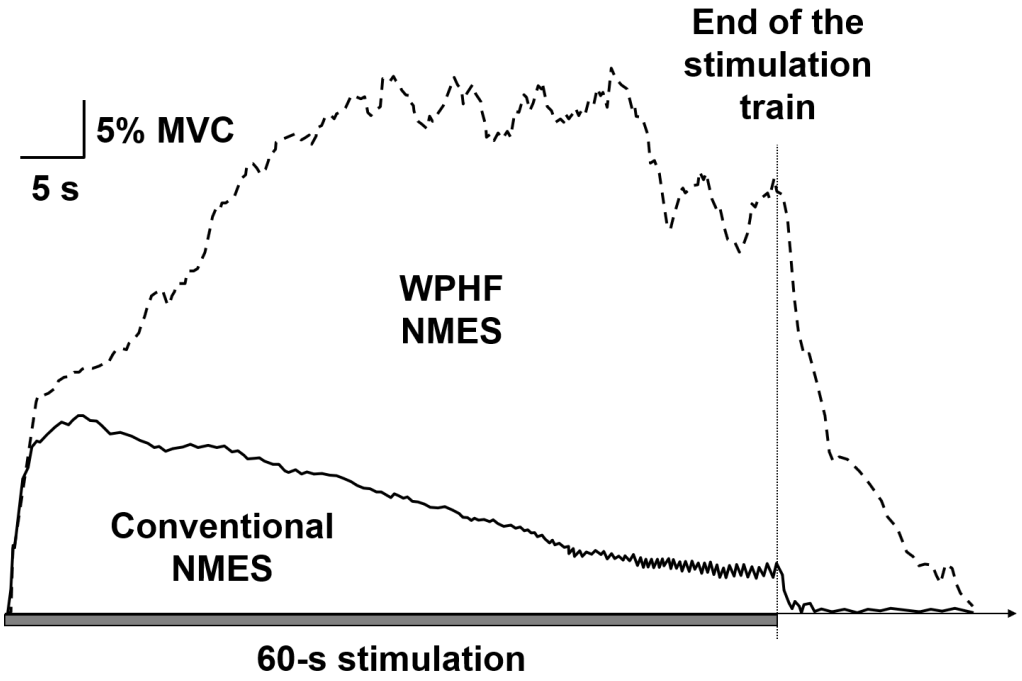

Figure 1.8: Representative exemplary force traces detected by the biceps brachii muscle of a healthy subject during the conventional NMES in solid line (100 µs pulse width, 25 Hz, 50 mA.) and the WPHF stimulation in dotted line (1 ms pulse width, 100 Hz, 6 mA).

1.2.3 Interleaved stimulation

Interleaved stimulation (iNMES) has been developed with the aim of lowering the discharge frequencies and recruiting different MU pools with whatever other stimulus pulse to reduce muscle fatigue. Stimulating impulses are alternated between muscle stimulation and nerve stimulation (named respectively mNMES and nNMES in several studies) [53], [54]. mNMES and nNMES recruit different populations of MUs (Fig. 1.9 B, C, D), at least with moderate-to-less excitement intensity [55], [56]. The amount to which iNMES reduces fatigue will depend on the degree of "overlap" among the MUs recruited by mNMES and nNMES [57]. Every studies found larger evocable M-waves even in depth, and the overlap of MUs recruited increase with rising in stimulation intensity.

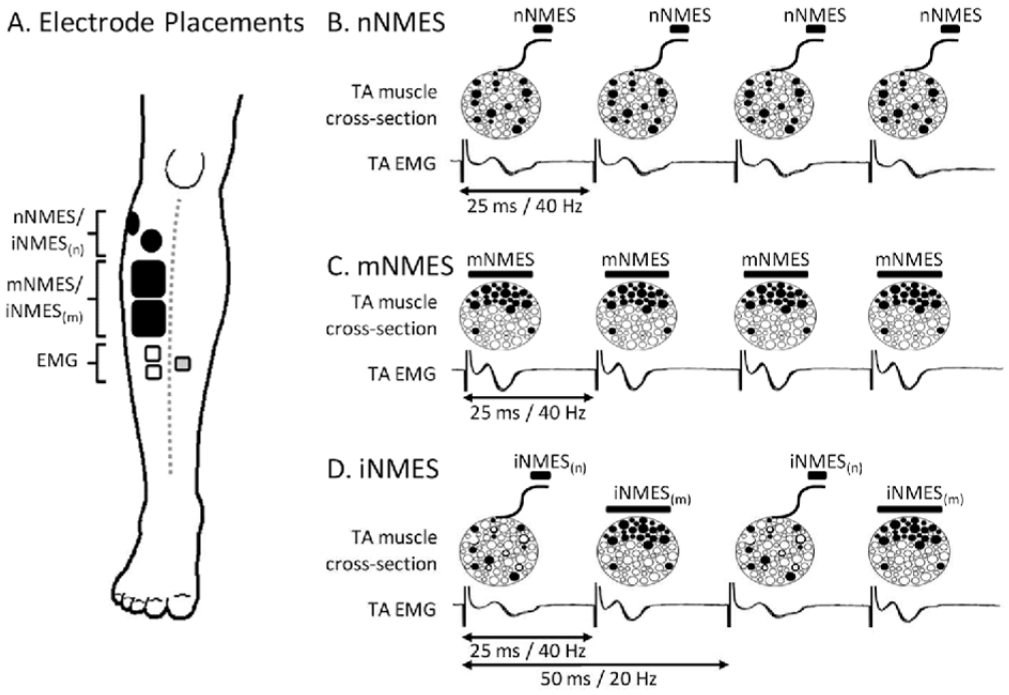

Figure 1.9: Example of electrode placements (A) over TA and the 3 methods of stimulation (B–D). It is also shown schemes of estimated spatial distributions of muscle fiber recruitment associated with each M-wave, where active and inactive muscle fibers are represented as filled and open circles, respectively. [53]

Regarding the discomfort associated with the two types of stimulation, they are both dependent by the injected current but it is often evaluated lower discomfort for the nerve elicited contraction, at comparable level. Also in this case the main drawback is the not easy accessibility of the nerve trunk for all muscles and consequently a selective stimulation of correct MN, that would not produce muscle co-activation. However, for example the TA is simple to elicit from common peroneal nerve, indeed it is the most studied for this kind of application (see paragraph 1.3).

1.3 Tibialis Anterior muscle

The Tibialis Anterior is a muscle which is part of the front muscles of the humans leg. It originates in the lateral condyle and proximal half of the lateral surface of the tibia and inserts into the medial and plantar surface of the medial cuneiform bone and the base of the first metatarsal bone (Fig. 1.10 A). It act on the ankle joint dorsiflexion, and assist in inversion of the foot. It is innervated by one of the CP nerve bifurcations: the deep peroneal nerve (Fig. 1.10 B) [58].

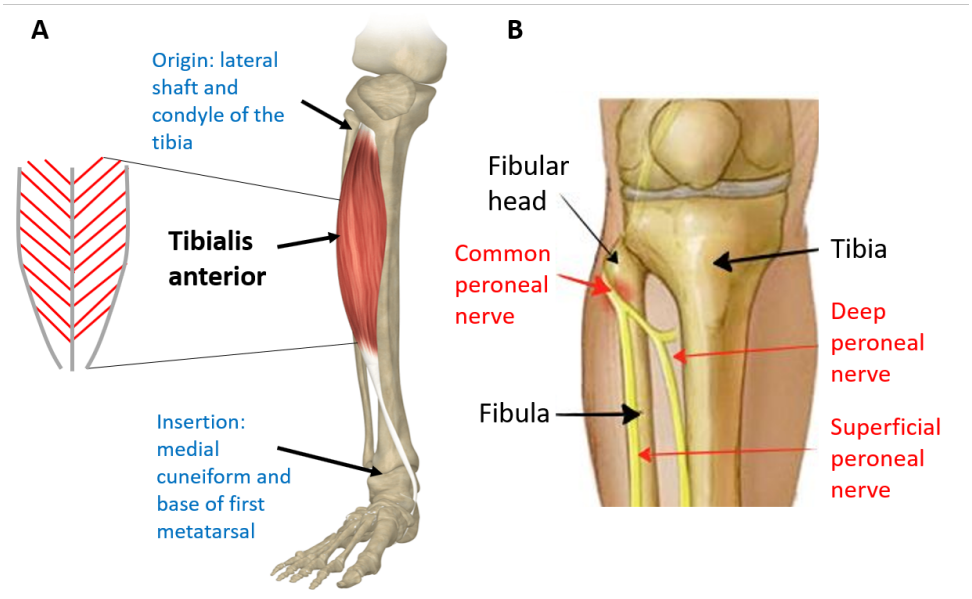

Figure 1.10: TA muscle and its pennated structure with the origin and the insertions highlighted (A), and the anatomy of the CP nerve (B)

As a skeletal muscle is composed of elongated muscle fibres grouped together in muscle fascicles surrounded by perimysium, or fibro-adipose septa. A thicker connective tissue sheath, the epimysium, surrounds the whole muscle. The main characteristic of such a muscle is that has their fascicles run oblique to the line of traction, and indeed it is considered a pennate muscles and in particular circumpennate or cylindrical [59]. Normal muscle fascicles are hypoechoic but become hyperechoic with fatty infiltration. Fibro-adipose septa, intramuscular tendons and aponeuroses and epimysium are hyperechoic. Fibro-adipose septa appear as linear, almost parallel bands of increased echogenicity on longitudinal scans [60] (Fig. 1.11).

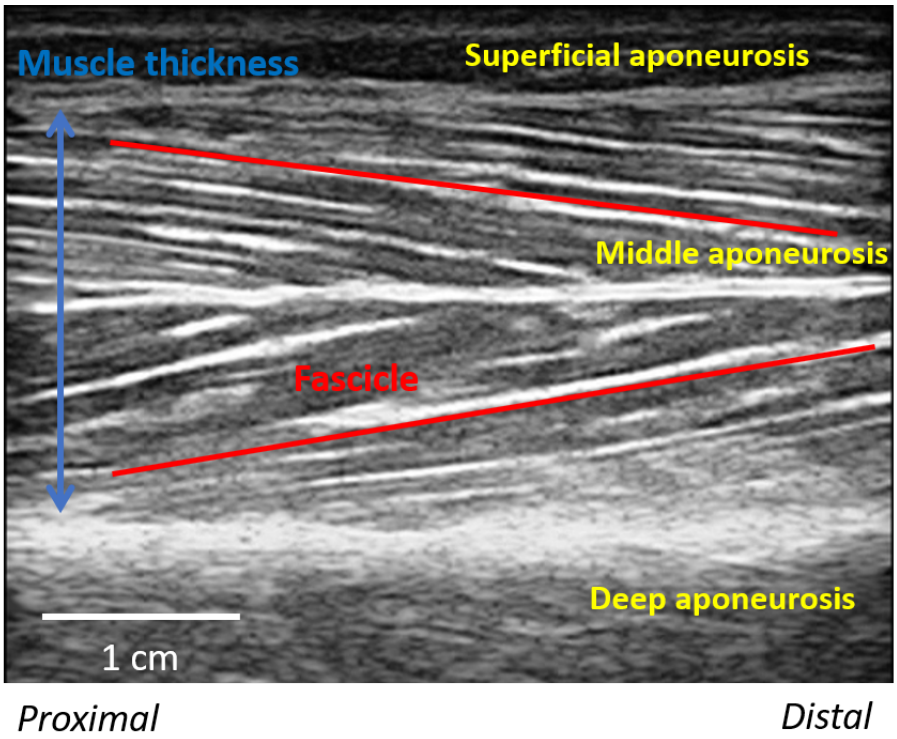

Figure 1.11: US longitudinal image of tibialis anterior.

1.4 Study objectives

The objectives of this study have been defined starting from the result obtained by Okuma, Bergquist, Collins, *et al.* in 2013 [61]. In this study the authors investigate the spatial distribution of MU pools recruited in the TA muscle by two application sites of electrical stimulation: over the muscle belly (mStim) and the CP nerve trunk (nStim). They shown that superficial MUs, those closest to the stimulating electrodes, are recruited preferentially during stimulation over a muscle belly; indeed for stimulation over the CP nerve trunk, it was found that recruited MUs were randomly distributed evenly throughout the muscle regardless of stimulation amplitude. To obtain this result, EMG was detected from superficial and deep regions of TA using fine-wires electrodes and then the maximal M-wave was measured to describe recruitment curves of the two muscle regions for both stimulation sites (Fig. 1.12). A possible limitation of this study was the limited sampling volume of a wire electrodes (i.e. detecting single or few MUs), whose detected signal may not be representative of the whole muscle in such a case (Fig. 1.13). In fact, the TA presents two compartments (i.e. superficial and deep) both with a pennated architecture. Hence MUs are scattered through the muscle and EMG potentials generated in specific muscle regions can not be registered by electrodes located in a different muscle location [62].

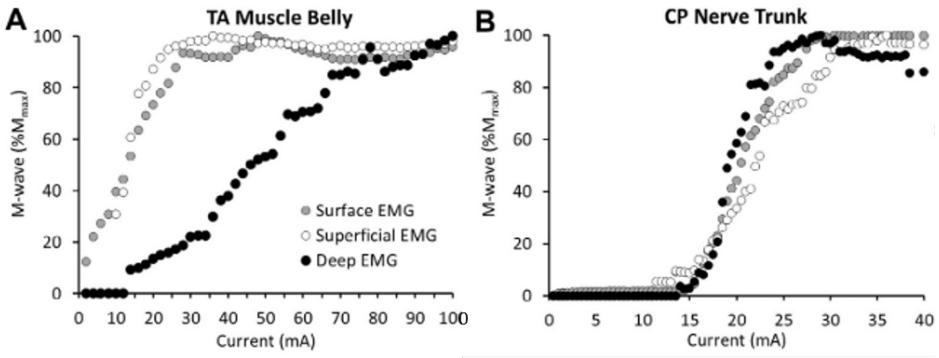

Figure 1.12: Recruitment curves as detected by surface and wire electrodes inserted in the superficial and deep TA compartment, for each stimulation site: over the TA muscle belly (A) or CP nerve trunk (B) [61].

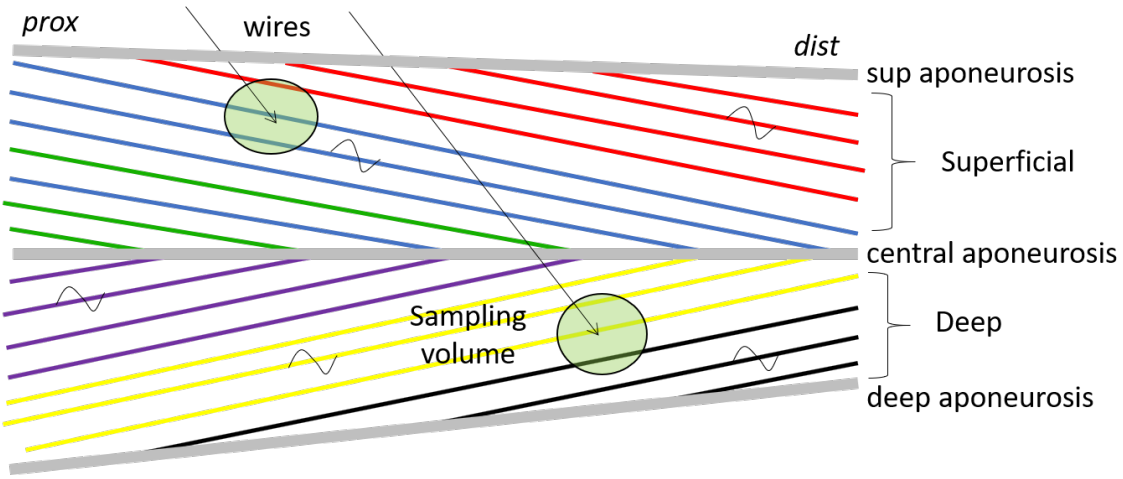

Figure 1.13: Schematic representation of the TA architecture in the longitudinal plane with two wires insert for each muscle compartment (i.e. superficial and deep). The colour of the fibers represents different MUs. It is illustrated how the signal detected by individual wires volume may not be considered representative of the whole muscle because some potentials can not be sensed by wire electrodes.

Although limited in terms of sampling volume, needle EMG is the only possible approach allowing for the sampling of deep EMG sources. Indeed, from surface EMG it is not possible to separate surface and deep sources contributing to the interference signal. An alternative approach to measure the activation of both superficial and deep muscle compartment is the ultrasonography which, instead of measuring the electrical potential associated with a MU activation, it quantifies the resulting tissue displacement. Therefore, this study does not focus on the electrophysiology of the electrically-induced contraction but instead on the biomechanics of TA and in particular the architectural changes of the muscle. We specifically aimed at characterizing the recruitment of superficial and deep TA compartments by evaluating morphometric parameters of skeletal muscle, such as Muscle Thickness (MT), Fascicle Length (FL) and Pennation Angle (PA). These parameters are of great interest to understand muscle activation as they described the biomechanical behaviour of the muscle which is closely related to the output force generated by such a muscle (i.e. ankle dorsiflexion): the shortening of pennated fibers pulls the tendon (i.e. aponeurosis) which in turn generates the movement of the ankle [63].

1.4.1 Hypothesis

In this study we hypothesized that muscle stimulation (mStim) activates preferentially the superficial compartment, instead nerve stimulation (nStim) activates both superficial and deep compartments, similarly to what happen during voluntary contractions. These hypothesis will be tested by measuring Muscle Thickness (MT), Fascicle Length (FL), Pennation Angle (PA) (for both compartments), from US images detected in the three different experimental condition.
Fig. 1.14 shows the expected behaviour of the considered biomechanical variables, according to our hypothesis:

- mStim would activate the upper region of the muscle and so the PA, and the MT would rise and the FL would decrease only for upper compartment;
- conversely Vol and nStim contractions would activate both compartments evaluating a rising in PA, MT and a lowering in FL of those.

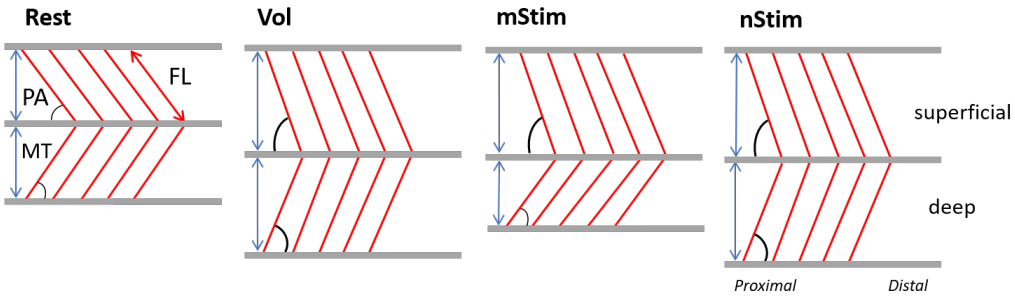

Figure 1.14: Schematic representation of the analysed muscle (fascicle in red, aponeurosis in grey) in three different condition, with reference to rest: Vol, mStim, nStim. It is highlighted the difference of pattern in the mStim between superficial and deep compartment.

Chapter 2

Materials and Methods

2.1 Experimental setup

In order to verify the study hypothesis, the experimental setup schematically described in Fig. 2.1 has been defined. The setup included the following instrumentation:

- Neuromuscular electrical stimulator;
- Ultrasound equipment;
- Electromyography (EMG) recorder;
- Force recorder.

2.1.1 Force recording

In this study the effect of different stimulation modalities on TA architecture was performed in isometric contractions for specific force levels. For this purpose, an isometric brace (OT Bioelettronica, Torino, Italy) housing a footplate connected with a force transducer (MODEL TF 031, CCT Transducers, Torino, Italy) was used to securely block the foot (Fig. 2.2 A, E). The way of blocking was important to ensure appropriate measurements of the isometric torque by the load cell with

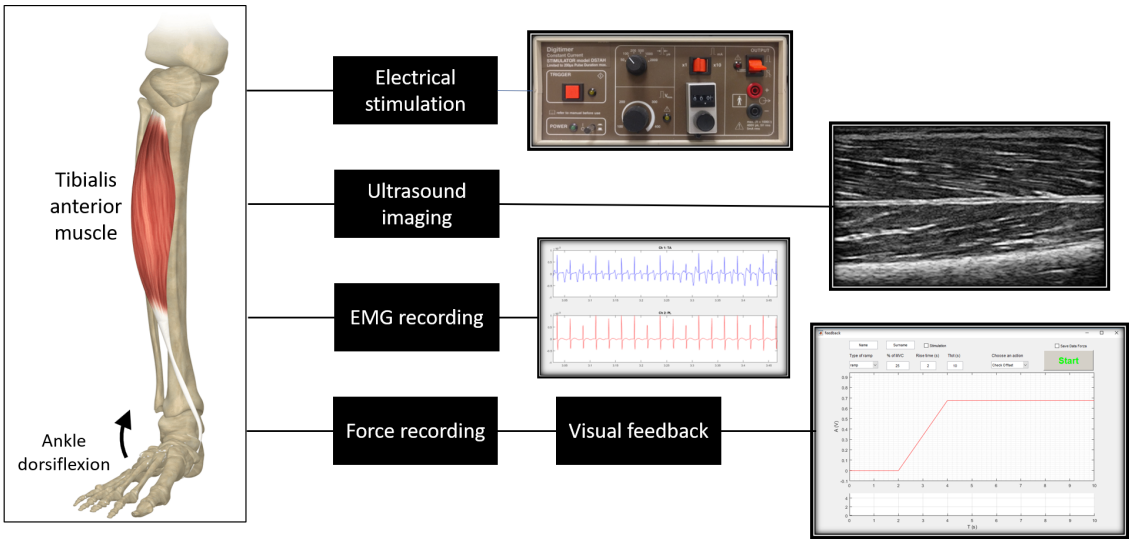

Figure 2.1: Scheme of the study application with all covered fields (black squares) that defines measurement on the subject (and its TA muscle).

bridge output fixed below the footplate. Thereby a single strap would not sufficient to immobilize the foot and so two home-made blocking bindings was designed and constructed (Fig. 2.2 B). The output of the load cell was amplified with general purpose amplifier (Forza, OT Bioelettronica, Torino, Italy) and acquired through a standard acquisition board (NI USB-6210, National Instruments, Austin, Texas) (Fig. 2.2 D, C).

The amplifier output has been checked with an oscilloscope in term of linearity using known sample weights lean on the footplate. The load cell has a Full Scale of 100 kg while Forza amplifier has a range of 0-5 V with an offset measured with the oscilloscope at about 2.78 V; in this way it is possible to evaluate traction (i.e ankle dorsiflexion) in the range between 0 and 2.78 V but also compression (i.e ankle plantaflexion) from 2.78 up to 5 V. Furthermore, Forza amplifier has the possibility to annulate the offset whenever need and also to set a gain from 100 to 1000. Following the formula in the Forza data-sheet (Eq. 2.1.1), given a gain of 500 and a sensibility of the load cell of 1.989 mV/V, it was possible to extract the force in kilograms. Knowing also the distance between the point of application of the load cell and the hypothetical projection of the ankle rotation point (about 13 cm), the

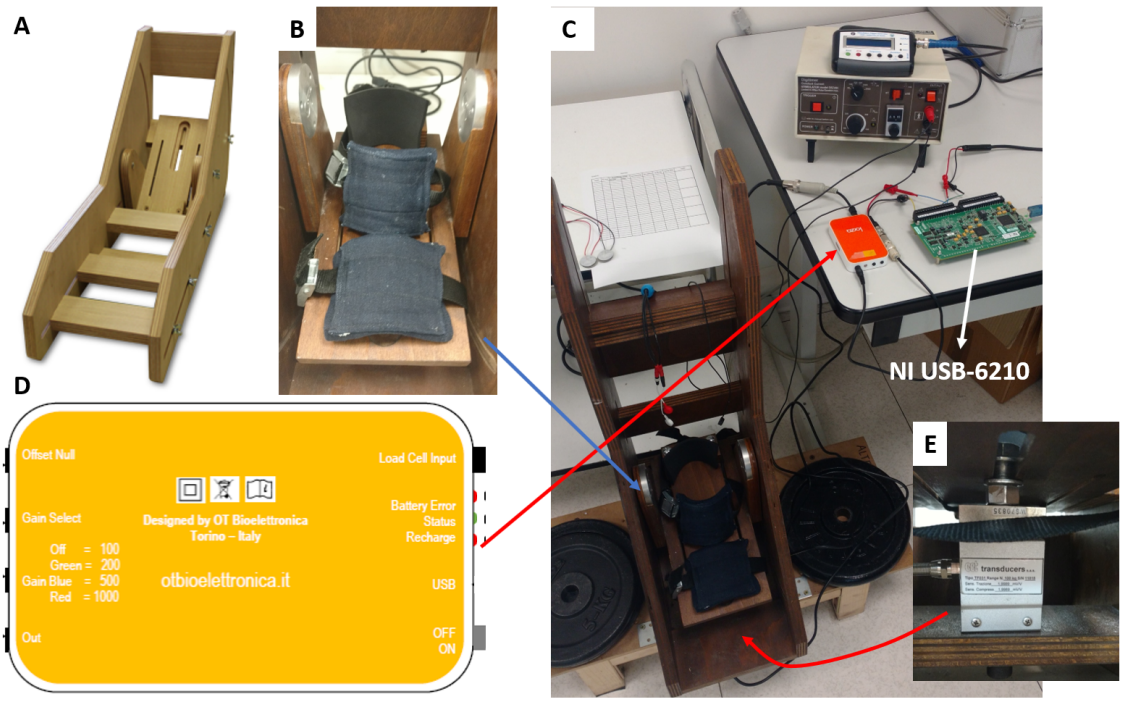

Figure 2.2: Isometric brace (A), two blocking bindings (B), Forza amplifier (D), mounted setup for force measurement (C), force transducer (E).

torque could be estimated (Eq. 2.1.1). Finally, with a gain of 500, the maximum traction force registered can be about 55.6 kg, corresponding to a torque of about 70.9 Nm. In this way, it was avoided saturation of amplifier during ankle dorsiflexion torque measurements in agreement with studies of Moraux, Canal, Ollivier, *et al.* that evaluate the MVC in this kind of isometric application [64].

$$F[kg] = \frac{V_{out}[V] * FS[kg]}{S[mV/V] * 5[V] * G} \tag{2.1}$$

$$V_{out} = V_{misurata} - V_{offset} \tag{2.2}$$

$$T[Nm] = F[kg] * g[m/s^2] * b[m] \tag{2.3}$$

2.1.2 Electrical Stimulation

For what concern the electrical stimulation of TA muscle, two main materials have been addressed: stimulator and electrodes. After that, a study on the stimulation methods has been thorough, in particularly for the localization of MPs and course of the nerve.

Stimulator A constant-current neuromuscular stimulation (model DS7AH; Digitimer, Welwyn Garden City, UK) was used (Fig. 2.3 A). For both mStim and nStim, a monophasic, rectangular pulse with 100-µs duration was used. This kind of pulse duration would preferably elicit MNs rather than nociceptors and in generally afferents. The stimulator imposes a current on the load modulating the voltage in order to have the desired current so that does not depend on the load provided that the required voltage is within the high-voltage power supply of the device (-150 ÷ +150 V). Since the load, i.e. the stimulated muscle, depends on the position of the electrodes, their size and the characteristics of the tissue, a constant-current stimulator is preferable to voltage stimulator. The stimulation frequency was finally set at 40pps through a stimulation trigger generator (StimTrig; Lisin, Politecnico di Torino, Italy) connected to the trigger input of the stimulator, to obtain a tetanic activation of the muscle with appropriate stimulation amplitude induced to reach a required force level.

Electrodes Two types of electrodes (Fig. 2.3 B and C respectively) were evaluated for this study: standard disposable adhesive snap electrodes (EB Neuro S.p.A., Firenze, Italia) and modified US transparent electrodes (bEMG-US; Lisin, Torino, Italy [65]). Standard electrodes was used for both mStim and nStim, while US transparent electrodes was used in a preliminary study to evaluate the effect of intra-electrodes distance for mStim. Modification of the bEMG-US electrodes consists in an adjustment to use these for stimulation instead of EMG detection, that is an halving of the electrode (Fig. 2.3 C).

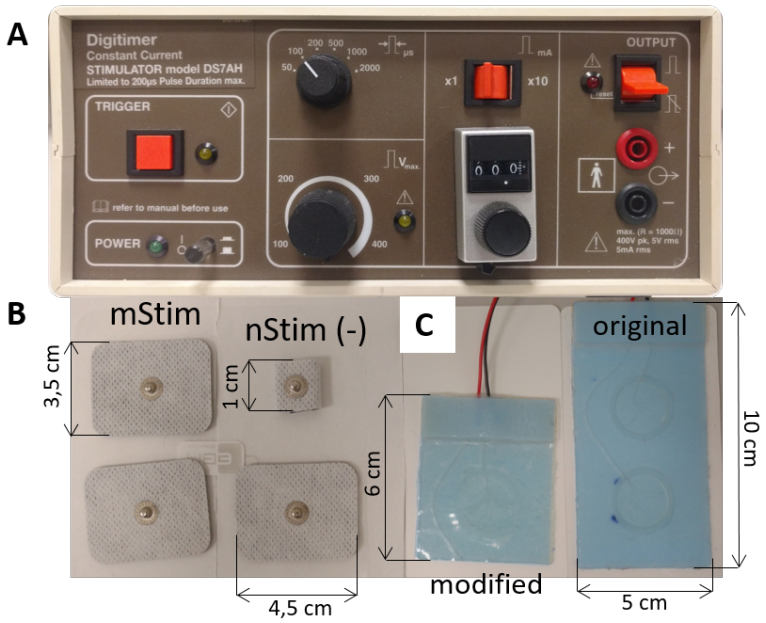

Figure 2.3: Constant-current stimulator panel (A), 3 snap adhesive electrodes used for mStim or as dispersive electrode for nStim, 1 trimmed snap electrode used as active pole for nStim (B) and US transparent electrode in modified and original version (C).

Motor points identification The main MPs, in subjects, for mStim were identified following the procedure described in Botter, Oprandi, Lanfranco, *et al.*, 2011. For the investigation of the TA, MPs identification were made while subjects were seated, with the knee at approximately 90 degrees and the ankle at 105 deg (Fig. 2.4 A). The muscle MPs correspond to the locations of the skin area above the muscle in which a twitch is evoked by an electrical pulse with the least injected current; the twitch is determined by manual palpation and visual inspection of the muscle and movement in proximal or distal muscle tendon. Scanning the skin surface with a small stimulation pen electrode (negative, cathode) and with a large dispersive electrode (positive, anode) placed opposite to the active electrode, to close the stimulation current loop (monopolar stimulation), the locations were identified slowly increasing the stimulation current (starting from 1 to 2 mA) until a clear muscle twitch could be observed.

Nerve course identification For what concern the nerve course identification, there is not a standardized procedure, and therefore other problems must be taken in consideration. First of all, the stimulation of the CP nerve it is not selective for the TA activation, since it may activate also the Peroneus Longus (PL), which has a force generating ankle eversion, and so act as antagonist for the dorsiflexion we want to evaluate. For this purpose, an EMG analysis can be added taking differential signals from these two muscles. In fact, the nerve identification was originally made looking at anatomical atlas and then with similar procedure of the muscle MPs. Using the pen as active electrode and a large electrode above nearest bony protrusions (i.e. patella), we identified the main nerve trunk. When a preliminary position was found, the active pole was substituted with a square adhesive electrode (1 x 1 cm) and then the muscle twitch re-checked. EMG are vary helpful on the identification of M-waves in TA and PL and gives a further checking of the stimulation. The aim was to visually evaluate the ratio of M-waves amplitude between TA and PL, and modifying the pressure on the active electrode (using an elastic strap) but also the orientation, to change the current lines above it and obtain a good stimulation. If the M-waves detected on TA was at least 3 times higher than that on PL as shown in Fig. 2.4 B, the stimulation was considered enough selective to obtain ankle dorsiflexion with none or minimal eversion.

2.1.3 EMG recording

A EMG probe (DuePro, OT Bioelettronica, Torino, Italy) with two bipolar signal was used to recorder activity over TA and PL muscles. With Due probe the user can visualize (in real time) and acquire data to store for further analysis. The electrode positioning (Fig. 2.4 A) was limited by other setup components (particularly for TA), however it may follow the indication of muscle innervation zones [66]. As mentioned in the previous paragraph, surface EMG is a helpful tool for checking the selectivity of the nStim over CP nerve. Beforehand, for this type of stimulation, operators checked the ankle movements only with visual inspection, in a way that no or minimal ankle eversion was visible during stimulation. We believe that this further checking is more quantifiable though it presents troubles considering the

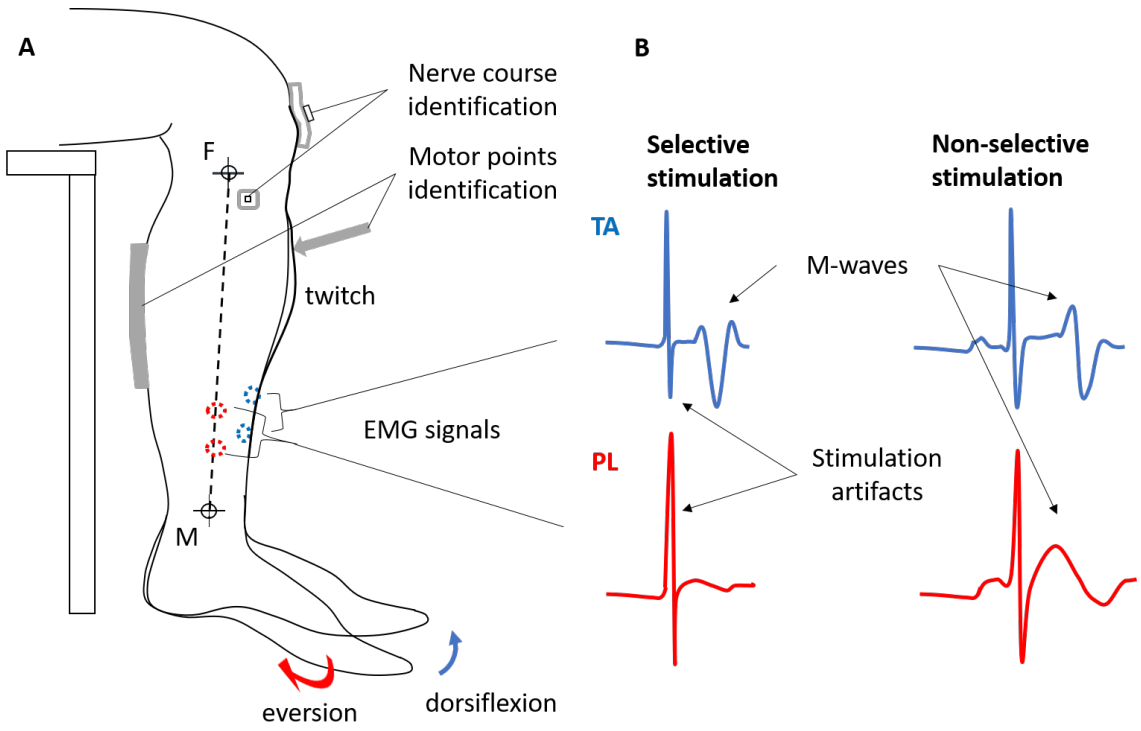

Figure 2.4: Setup for identifications of TA MPs and CP nerve course (A). Example of EMG single M-waves taken from single differential of electrodes on TA and PL.

fact that amplitude of the M-waves registered after a stimulation pulse depends by several factors such as location of sampling electrodes or inter-electrodes distance. The cross-talk effect, which can corrupt the signals, must also be taken into account due to the proximity of considered muscles. In fact, a surface EMG signal detected on the skin above TA and of a signal registered above the neighbouring PL may be due to cross-talk rather than to real activation of the muscle below the electrode [67], even if one of the muscles are considered silenced. Therefore, since the protocol stimulation would be at 40 pps, further analysis at this frequency must be taken into account. In fact, an increase in frequency together with the rising of the stimulation intensity compared with those used for the above mentioned identification, would increase the possibility to elicit undesired M-waves. In Fig. 2.5 it is shown a situation of EMG original signals taken from a representative subject stimulated ad 40 pps, where basically there are no M-waves present on PL.

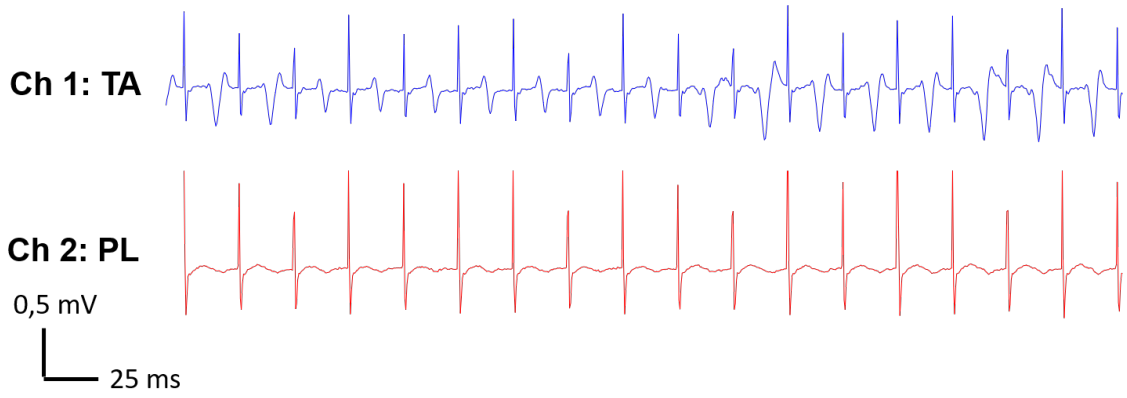

Figure 2.5: Original single differential EMG traces of TA and PL of representative subject. Artefacts and subsequent M-waves occurs every 25 ms (40 Hz stimulation frequency). As we can see in the increasing of M-wave amplitudes, the injected current increased but still the stimulation remains selective for TA.

2.1.4 Ultrasound imaging

A MyLab X Vision ultrasound device (Esaote, Genova, Italy) equipped with a linear-array transducer (code LA532, width 5 cm) with variable frequency 3–13 MHz, set to 7.5 MHz to analyze skeletal muscle, was used to scan the TA (Fig. 2.6 A). Gain, depth, focus number and position was evaluated initially to achieve good quality of images. When good system-setting was found, all parameters were kept constant except for the scanning depth and the gain that could be adapted to subjects. The idea for protocol application was that several videos would be recorded at the sampling rate of 20 frames/s and then transferred to a workstation for offline processing and later analysis (see paragraph 2.2.3). For what concerns the ultrasound probe positioning, several tests were made to define the best position and orientation allowing the definition of the anatomical structures such as superficial, central and deep aponeurosis and fascicle orientation. An example of the probe positioning is shown in Fig. 2.6 B.

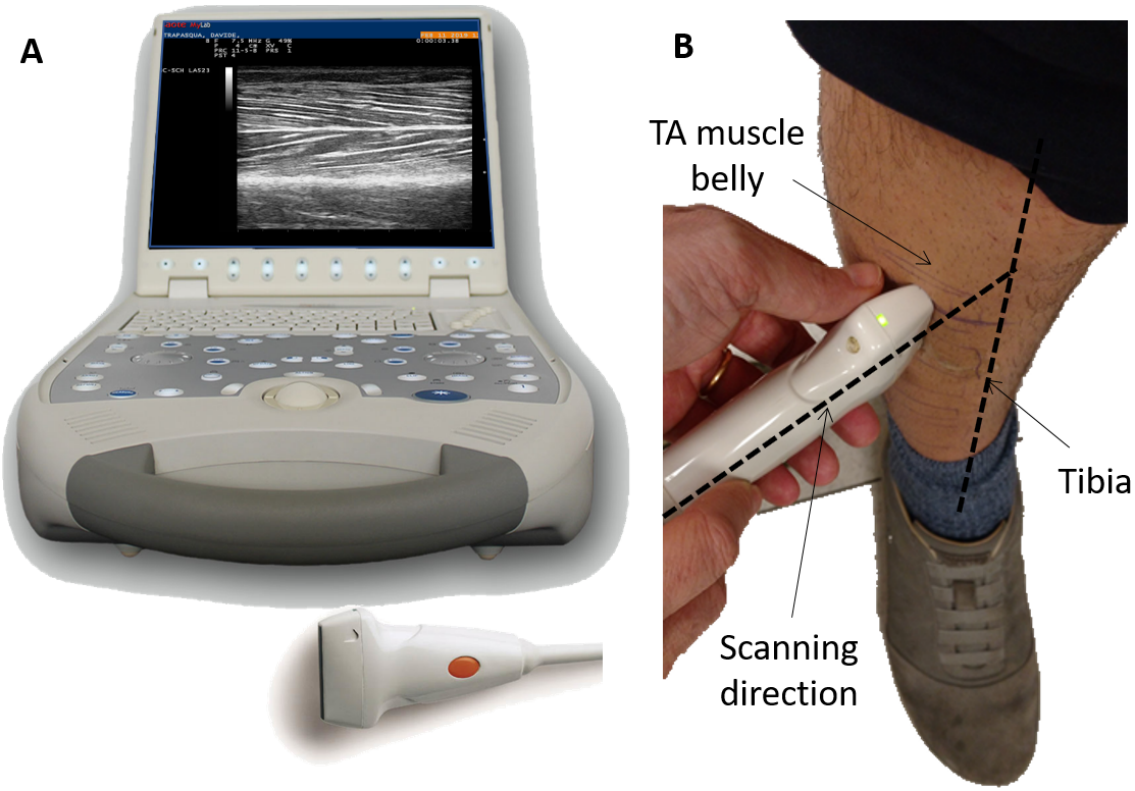

Figure 2.6: MyLab X Vision US device with the linear probe (A); example of probe orientation on the subject (B).

A good image was defined as the one that allow to visualize the middle and deep aponeurosis, as well as individual fascicles in both superior and inferior muscle compartments (see Fig. 1.11 paragraph 1.3). The scanning direction defined by probe orientation is a relevant factor affecting the image quality. Specifically, the US beam should be perpendicular either to the middle and deep aponeurosis. This is not always possible due to personal anatomical conformation of the TA and therefore a good compromise may be found. In same cases, for instance, the two aponeurosis are not parallel to each others, thus making impossible a perpendicular crossing of the US beam through both of them. It is also important to note that the tibia bone is in close proximity with the deep aponeurosis. A preliminary transversal scan as in Fig. 2.7 allow to evaluate an hypothetical longitudinal direction, taking care not to tilt the probe excessively towards the tibia, that blocks the thickening of the muscle.

However, the position of the probe is limited by the other components of setup, such as electrodes (specially those for mStim) that are placed just above the muscle. As already mentioned, US transparent electrodes were used in part of the experiments. In this case, the probe was sticked to the electrode previously bonded on the skin, and then to adapt the position and orientation became quite difficult. Moreover, the use of this kind of electrodes requires an increase in power and gain to obtain good image quality. In any case, it is necessary to underline that there is a large variability among different subjects due to anatomical conformation, and so every subject may be specifically analysed in probe position and orientation to achieve the required quality.

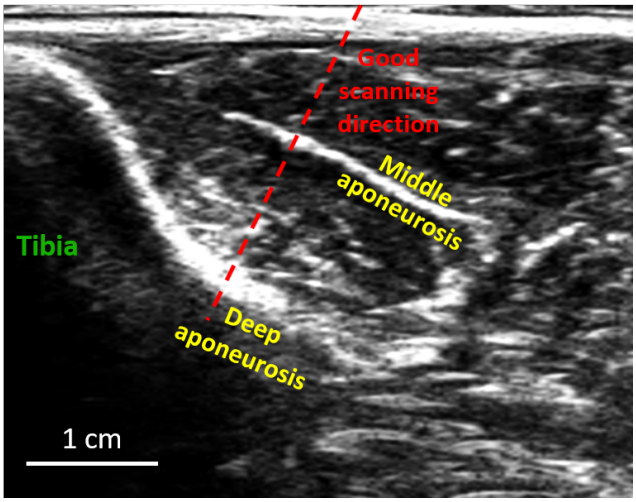

Figure 2.7: Transversal image of TA to visually inspect the scanning direction to achieve good quality in longitudinal image.

2.1.5 Visual feedbacks

As described above, all the consideration in muscle architecture (and on its change) are made for specific contraction levels which are kept constant for different contractions in order to be able to compare the variables of interest for the same force output (like-with-like comparison). For this reason we measured the force and we display the measured values as a feedback for the subject or for the experimenter.

The force trace registered (see 2.1.1) was displayed in real time for feedback purposes on a computer screen, along with the required force profile, that is a 2-s ramp and a plateau level of 5 seconds. A custom-written MATLAB Graphical User Interface (The Mathwork, Natick, MA, USA) was used for this purpose (Fig. 2.8). The plateau level of the ramp could be defined on the GUI in terms of percentage of MVC level, therefore the interface presents a functionality to record this measure (i.e MVC). For our purposes two target level correspondent to 15% or 25% MVC were chosen. This force visual feedback would be useful to an experienced subject during voluntary contractions that has to reach the target force (either 15% or 25% MVC) in the 2-s ramp and keep this force constant for the remaining part of the ramp, but also for the experimenter that manually change the stimulation current in order to match the required force profile during mStim and nStim.

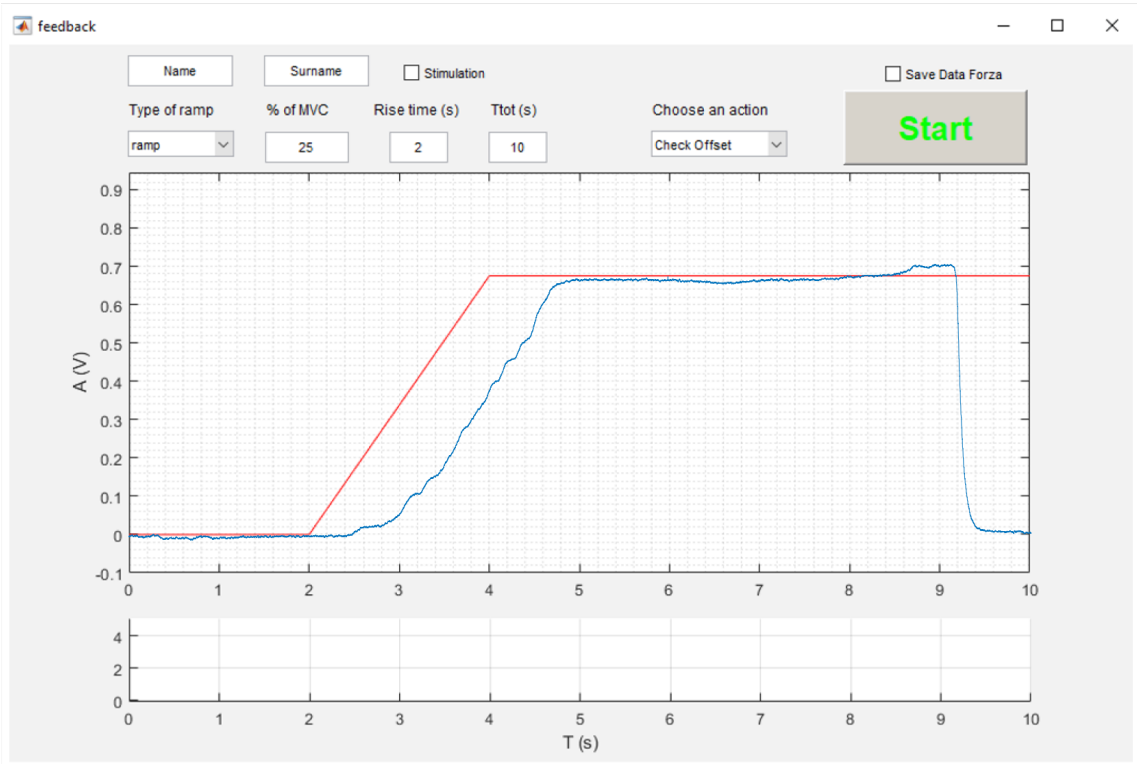

Figure 2.8: Matlab Graphical User Interface with target ramp profile (in red) and real force signal superimposed (in blue).

2.2 Protocols

For this study two protocols were carried-out: a preliminary one and a final one. As already mentioned in the *Study objectives* (paragraph 1.4) the main aim is to verify whether mStim and nStim can activate different portions of muscle. In Fig. 2.9 A is shown a scheme of the experimental setup for the definitive study, instead Fig. 2.9 B has two pitch of the mounted setup for mStim (one the right) and for nStim (on the left) in real subjects. However, the preliminary study was specifically done to asses the effect of electrode distance in mStim and for this purpose US transparent electrodes was necessary. The only difference in this protocol regards the positioning of electrode (Fig. 2.9 C); the idea was to use the transparent electrode for a Short mStim and move distally the other electrode to achieve a Large mStim.

For nStim, we positioned a large anode (3.5 $\times$ 9 cm) over the lateral aspect of the patella and a small cathode electrode (2 $\times$ 2 cm) over the CP nerve trunk, approximately 1 cm distally with respect to the head of the fibula along the path of the CP nerve (see paragraph 1.3). As already explain, the peroneal nerve stimulation may activate both TA and PL, hence we carefully adjusted the cathode position in order to achieve a selective TA stimulation (i.e. pure ankle dorsiflexion).

For mStim, the cathode electrode (3.5 $\times$ 4.5 cm) was positioned over the most proximal motor point, while the anode electrode with the same size of the cathode was attached about 10 cm distally with respect to the cathode (in the definitive study).

While, in the preliminary study, the transparent electrode (5 x 6 cm) that act as anode for mStim Short, was positioned about 6.5 cm distally to the same cathode as before; then an anode for mStim Large was positioned about 6.5 cm distally again. Obviously these positioning measures are indicative because they could vary according to the subject.

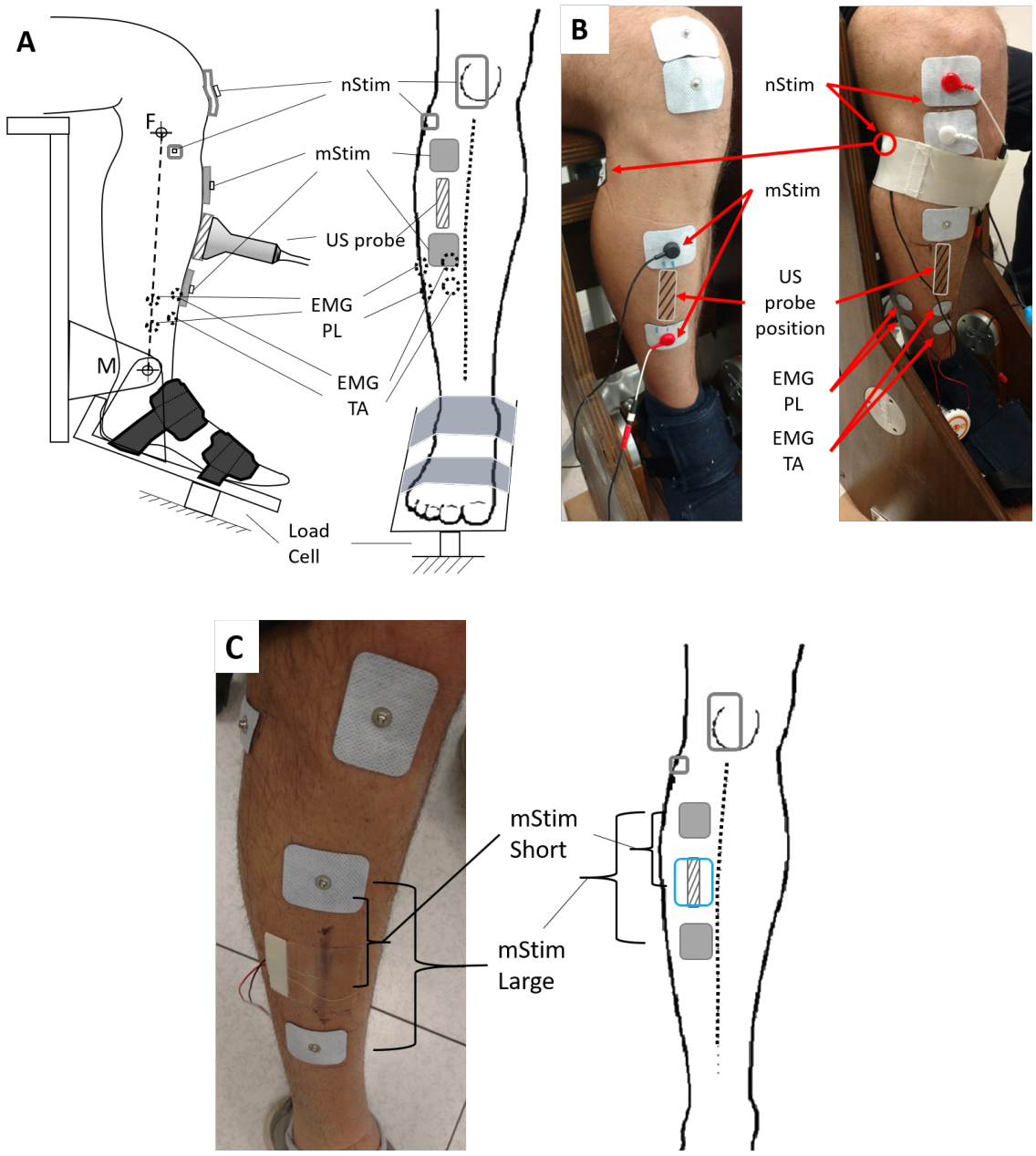

Figure 2.9: Schematic setup positioning in lateral and transversal view (A); real setup positioning on two subjects, one for "normal" mStim and the other for nStim with also EMG electrodes (B); electrodes positioning for mStim Short and Large in real and schematic view (C).

2.2.1 Subjects

Two male participants (age range: 24–38 years; height: 177.5 ± 3.5 cm; weight: 67.0 ± 2.8 kg) for the preliminary study and nine participants (age range: 24–45 years; height: 177.9 ± 8.7 cm; weight: 67.6 ± 7.9 kg), two females and seven males were included in the final one. All subject had no history of neurological or musculoskeletal impairment or disease were recruited. The study was conducted in accordance with the Declaration of Helsinki and informed consent was obtained from all participants after receiving detailed explanation of the study procedures. Unfortunately, the experiment on the two tested female did not complete because of a good nStim condition (see paragraph *Nerve course identification* 2.1.2) was not achieved.

2.2.2 Experimental procedure

Participants were seated on a chair with backrest in front of the isometric brace. The position of the subject was adjusted to obtain approximately 110 deg of hip angle, 90 deg of knee angle. Ankle angle was 105 deg, as defined by the isometric brace settings. US images were detected from the TA during three types of isometric foot dorsiflexions at 15% and 25% of the MVC: voluntary (Vol), induced by NMES (mStim), and induced by nerve stimulation (nStim). For each contraction type and force level, two or three trials were acquired. At the beginning of each experiment, participants performed at least 2 MVC of ankle dorsiflexion, receiving visual feedback of their torque production on the screen and verbal encouragement. To sum up, during voluntary contractions the subject was asked to reach the target force (either 15% or 25% MVC) with a 2-s ramp and to keep this force level for 5s. The same force profile was used during electrically-induced contractions, in which the experimenter manually changed the stimulation current in order to match the required force profile. For each subject and stimulation modality, the appropriate amplitude inducing the required force level (15% and 25% MVC) was identified after the electrode positioning. A EMG registration at 25% of MVC in nStim was saved to be analysed later, after the identification of final electrode location that maximizing the M-wave detected from TA while minimizing that detected from PL.

2.2.3 Data analyses

The Muscle Thickness (MT) of both compartments was calculated from one frame of the video in rest condition and one during contraction, using a custom-made Matlab script to manually draw (using *imfreehand* function) three lines correspondent to superficial, middle and deep aponeurosis (see Fig. 1.11). Thereby upper and deeper MT can be evaluated as the superficial-middle distance and middle-deep distance of the drawn profile respectively. The metric used to calculate the distance between two profile curves is similar to the Hausdorff distance: minimal euclidean distances of each point of a curve from the other curve points are calculated and the other way around, and an average is made of all these minima (Hausdorff distance indeed take the maximum of the minima). In this way a representative mean distance of the two compartments is obtained. After that the percentage change between rest and contraction is computed.

Muscle Fascicle Length (FL) and Pennation Angle (PA) were estimated semi-automatically through a freely available software named *UltraTrack* (version 4.2 in Fig. 2.10) published by Farris and Lichtwark [68] based on affine transformation extensions to optic flow (affine optic flow algorithm by [69]). The validity and reliability of the affine optic flow algorithm of Cronin, Carty, Barrett, *et al.* was published in 2013 [70]. This affine optic flow model implemented in the main algorithm of the software, computes on consecutive images in the sequence the optic flow and the affine transformation. The model is based upon an affine extension of the well established Lucas–Kanade method [71].

First of all, it is necessary to crop the image and especially remove the edges above or below the image by removing the surrounding edges from the image (usually relative to the US device settings). The image scale (pixel / mm) is calculated by dividing the number of pixel lines by the specified image depth, which refers to the scanning depth in mm and is entered from the editable text box. In the first ultrasound image of each video sequence, an examiner selected the muscle Region of Interest (ROI) (upper and lower compartment) and drawn fascicles; at least two fascicle must be defined to obtain then an average of FL and PA. Clear oblique lines reflected by inter-fascicular connective tissue was identified as fascicles. The

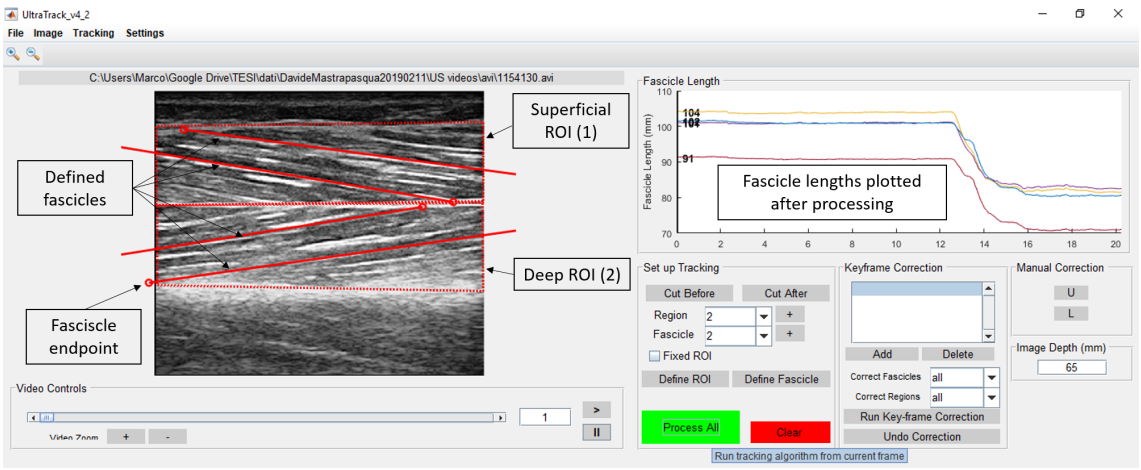

Figure 2.10: Snapshot of *UltraTrack* GUI. On the left panel there is the first frame of US video sequence with the regions of interest defined with red dotted line and two fascicles per region defined with red solid line in which the endpoints are represented with circle. The right down panel show some command buttons and settings instead the right top show the results of the tracking algorithm with the evolution of FL over time.

FL is defined as the length of oblique line from the superficial or deep aponeurosis to central aponeuroses, whereas the PA was defined as the angle between the fascicle selected for length measurement and the central aponeurosis [63]. ROI is referred to as the contour of the muscle cross-section, usually include the aponeurosis that borders the muscle. Both the ROI vertices and the endpoints of the fascicles have the affine flow transformation applied to them and for both they will move and change shape to account for movement of the muscle. Once the algorithm is run, FL are plotted in the axes at the top right of the user interface and it is also possible to see the tracked fascicle(s) and ROIs overlaid on every sequence image (Fig. 2.10).

Tracking data are saved as MAT file with all the necessary information. It should be noted that PA is actually the angle of the fascicle relative to the image horizontal axis and then a correction with the angle of the central aponeurosis must be taken in account. When the entire length of the fascicle was not included in the image, the length of the missing portion was estimated using linear extrapolations of the fascicle and aponeuroses. FL and PA for the upper and lower muscle compartments

were compared for different contraction types. Specifically, for each experimental condition we computed the percentage change of each variable with respect to the rest condition. It is worth noting that each session included a 5-s rest before the force development which persists for at least 5 seconds, therefore each contraction was compared with a rest condition recorded immediately before it. Even if the subject is theoretically motionless, an average of 2 seconds for the rest and contraction term was done to minimize the effect of possible probe movements during a session. In Fig. 2.11 are represented the tracking data (i.e FL and PA) over time for deep and superficial compartment in which the black lines highlight the 2 rest seconds and contraction seconds. Furthermore, probe movements is likely larger between sessions than within same session and so it is always necessary an initial rest condition.

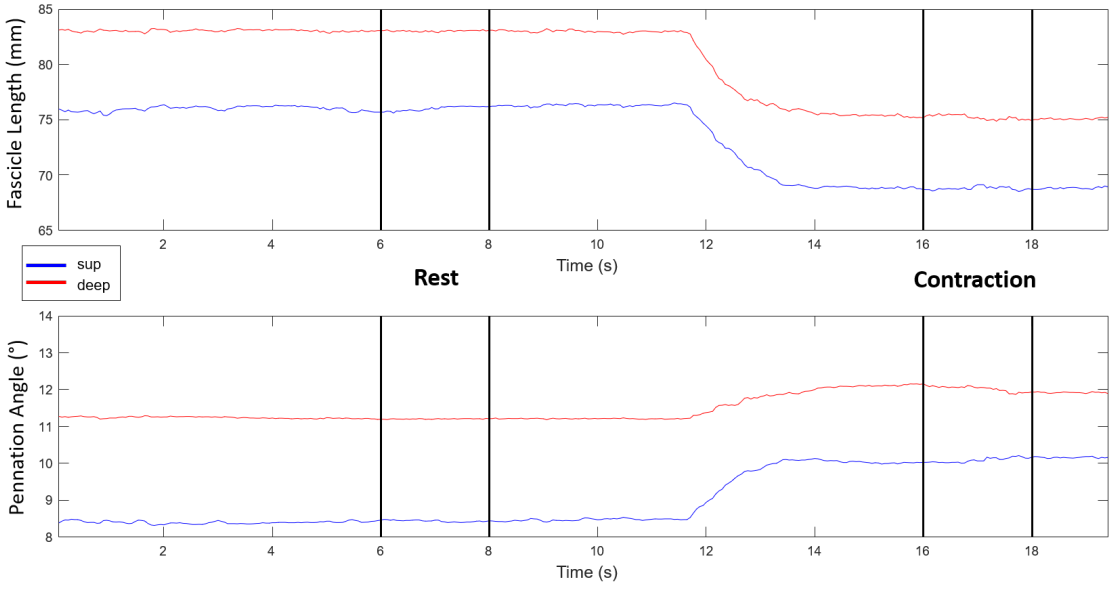

Figure 2.11: Example of plotted tracking data of a single trial of a subject.

Chapter 3

Results and Discussions

3.1 General description

All tested subjects completed the experiment, without reporting excessive discomfort. In two participants (TaPi) (FrSa), the ratio between the amplitude of EMG signals detected from TA and PL during nStim was not larger than 3, while for all the others we were able to selectively stimulate the TA evaluating enough larger ratio of M-waves (see paragraph 2.1.3). These data were confirmed by visual inspection and manual palpation of TA and PL during the test contractions to obtain ankle dorsiflexion with none or minimal eversion, prior to the beginning of each experiment. Current amplitudes (mA) required for any type of stimulation are reported in table 3.1 with mean and standard deviation of all subjects.

	mStim			**nStim**		
	Exc Thr	15%	25% MVC	Exc Thr	15%	25% MVC
Mean (mA)	32.14	56.14	72.14	17	21.67	29.37
Std (mA)	7.06	6.82	10.95	7.81	9.24	12.6

Table 3.1: Mean and standard deviation of stimulation current of subjects, required to obtain muscle activation (excitation threshold, Exc Thr) and reach the 15 and 25 % of MVC for both sites (i.e. nerve and muscle).

3.2 Ultrasound image quality

The image quality varied between subjects. The best position and orientation allowing the definition of the anatomical structures (i.e. superficial, central, deep aponeurosis and fascicle) may not always be the same during all the experiment. Wherever it was not possible to obtain an adequate definition of the anatomical structures, priority has been given to fascicles over aponeurosis. In fact, lower aponeurosis was the most problematic one in terms of definition. As already mentioned in paragraph 2.1.4, the US beam should be perpendicular to both aponeurosis, but the lower one was often too inclined with respect to the middle. This results in a blurred viewing of the deep aponeurosis that appears thickened (with respect to the central one). Moreover, due to architectural changes during the contraction it is possible that a good definition of deep aponeurosis during rest condition changes in the contraction phase (Fig. 3.1). In all subjects considered, we found sufficient image quality at least with regard to the identification of muscle fascicles.

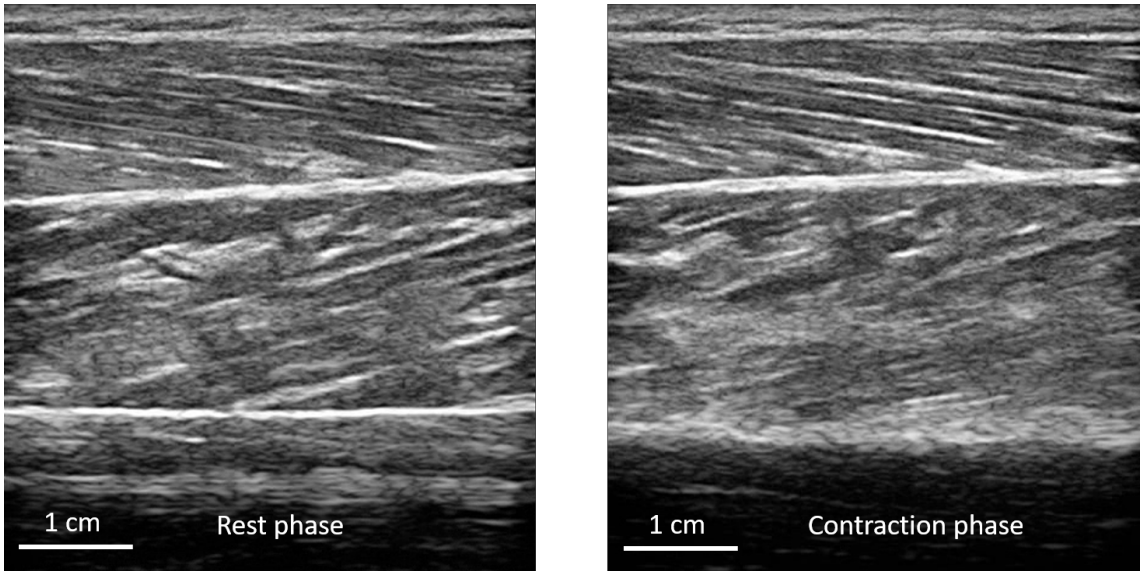

Figure 3.1: Comparison between rest phase (on the left) in which all aponeurosis appear more clearly than in contraction phase (on the right) where the deeper aponeurosis is blurred.

In 4 subjects (AlBo1) (MaCa) (NiMa) (AlBo2) lower definition was noted for deep aponeurosis during contraction phase in comparison with that of rest (consequently the FL may be of difficult interpretation). Instead, in 1 subject (HeCa) a worse definition of central aponeurosis during rest phase in relation to the contraction phase was necessary to better visualize fascicle during whole test. In same videos of 1 subject (StBe), central and deep aponeurosis were not clearly defined during the test despite the fact that there was a very good definition of the fascicles in both compartments for the total duration. In any case, all this indicates that the deep compartment was more problematic in terms of image quality, and therefore this may lead to errors in the evaluation of the variables of interest for this portion. However, all videos were checked also with the Tracking algorithm (paragraph 2.2.3). The ROIs representing TA portions were identify in the first frame, together with two fascicles for each compartment. Once the program evaluated movements of ROIs and fascicles, the tracking data were checked if they seem to be as expected (see Fig. 2.11).

3.3 Effects on TA architecture

In order to have a global view of the effects of the contraction type (i.e. voluntary, induced by nStim and by mStim) on the architectural changes of TA, the results are represented in a Cartesian plane where the percentage change of FL and PA are reported in the x and y-axis respectively. Each graph reports the results for one contraction type. Therefore, each point represents a single trial, with the colour coding whether it was estimated from the superficial or deep compartment of TA. In this kind of representation, it is possible to visualize how the points are clustered differently in the FL-PA plane for different contractions and also note if the difference is more due to changing in PA or FL.

3.3.1 Preliminary results

The aim of the preliminary study was to evaluate differences with variable inter-electrode distance for mStim. Short and Large distances were tested as already explained. It was hypothesized that mStimLarge may activates more the deep portion due to a wider spread of current lines reaching even deeper nerve terminal branches. The graphs of the two subjects are shown in Fig. 3.2, in which can be highlighted the clustering of blue and red points similar for Vol and nStim in line with our hypothesis. This clustering is different compared to mStim but not real evidence show meaningful changes between Short and Large mStim. In the mStimShort graph of the first subject at 15% of the MVC it is not possible to note clusters fo the two portions of TA as well as for the second subject in the same condition. The same goes for mStimLarge at 25% MVC of the first subject. In view of these results, we are not sure of inter-electrode effects and it is also necessary to underline that the use of another electrode in the experiment, besides complicating the setup and protocol, enhance the inter-subject variability due to the electrode positioning. In fact, based whether the subject has a shorter or larger muscle, the stimulated portions will be different in any condition.

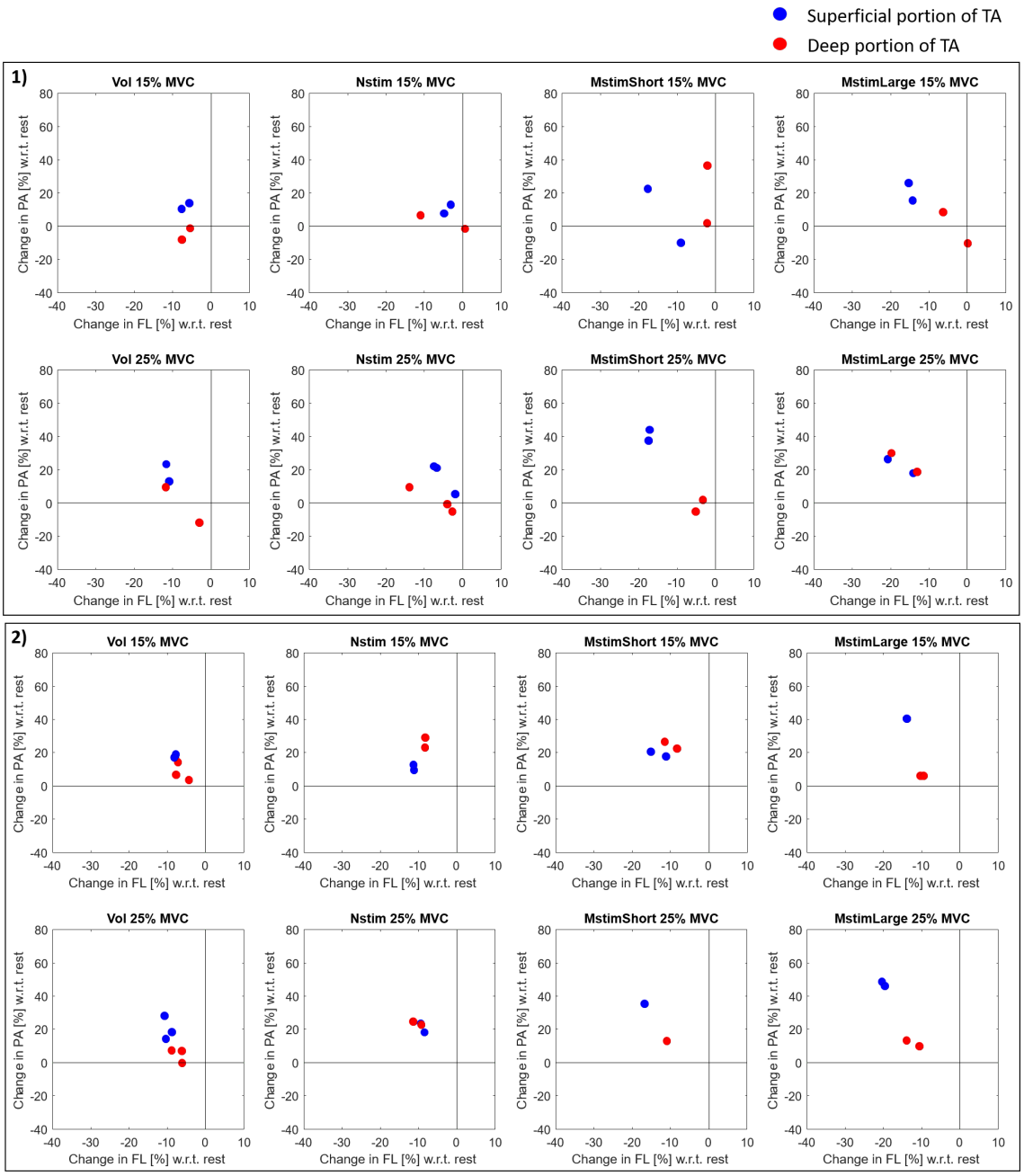

Figure 3.2: Preliminary results for subjects 1 and 2 in cartesian representation (x: percentage change FL), y: percentage change PA). There are not clear evidences showing meaningful variety between Short and Large mStim.

3.3.2 Final results

A representative subject is shown in Fig. 3.3 in the same Cartesian visualization described in the previous paragraph. The main evidence is in line with our assumptions, that is a similar clustering of points for Vol and nStim,which is different as compared to mStim. The differences between compartment in mStim are valuable mostly along the y direction, indicating that the PA of the superior portion increase more (of about 45%) than that of the deep one (of less than 20%). Another relevant difference is that the changes in FL (i.e. shortening) for both superficial and inferior compartment in case of mStim (about -20% with reference to the rest condition) is greater than those of Vol and nStim (about -10%). These behaviours are mostly observed for the contractions at 25% MVC and which is probably associated to the degree of recruitment, which is higher that at 15 %, implying a larger amount of architectural changes. With the use of only one electrode distance in the final study, the electrode positioning is mainly dependent by the obstruction of the US probe, however also in this case there may be inter-subject variability.

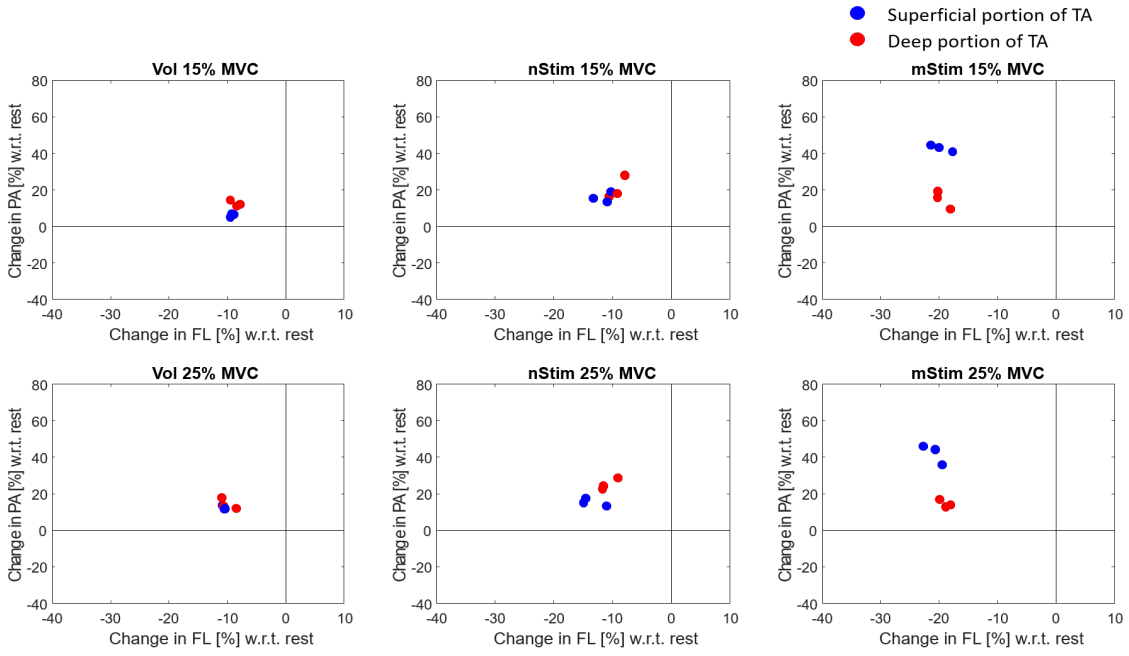

Figure 3.3: FL-PA graphics of a representative subject.

3.4 Statistical analysis

With data of the final study (7 subjects) and the preliminary study (2 subjects, taking only mStimShort as representative), we performed a statistical analysis to evaluate if our hypothesis can be confirmed. We extrapolated a mean of the trials for each stimulation type of every variables (i.e. MT, PA and FL) of both compartment and then percentage changes of those variables were calculated. In the way to represent each cluster viewed above before was described by 1 point for every subjects. Finally, we aimed at evaluating whether there was significant differences between contraction types for each variable for both MVC percentage. For this purpose, the averaged variables were analysed using repeated-measures variance analysis (within-subjects ANOVA) and then post-hoc test (*Bonferroni*) performed to find statistically significant differences between contraction types.

3.4.1 Muscle Thickness (MT)

We started to analyse the Muscle Thickness (MT) that can be considered as the first approach to understand differences in architecture during contraction type. Unfortunately, no significant statistical difference could be observed for both superficial and deep muscle portion as shown in Fig. 3.4. Perhaps the percentage change involved at this contraction level is very low (indeed evaluated mean of thickening/thinning is around 0) but there is also a great variability between subjects. In any case, we have to consider that MT is strictly dependent from the other two considered variables according to the formula $MT = FL \cdot \sin PA$ if the muscle model seen in paragraph *Hypothesis* 1.4.1 may be considered correct. Hence, MT will proportionately increase but also decrease depending on how much PA increase and FL decrease. For instance, if fiber shortens a lot (i.e. FL decline) but PA increases little, the MT decreases, conversely, if FL decreases little but leading to a major PA increase, the MT rises (Fig. 3.5). The relative changes of PA and FL due to a contraction, depend on several anatomical factors, e.g. the tendon stiffness. According to the formula $MT = FL \cdot \sin PA$, we evaluated the theoretical percentage change thickness to be compared with the experimental one.

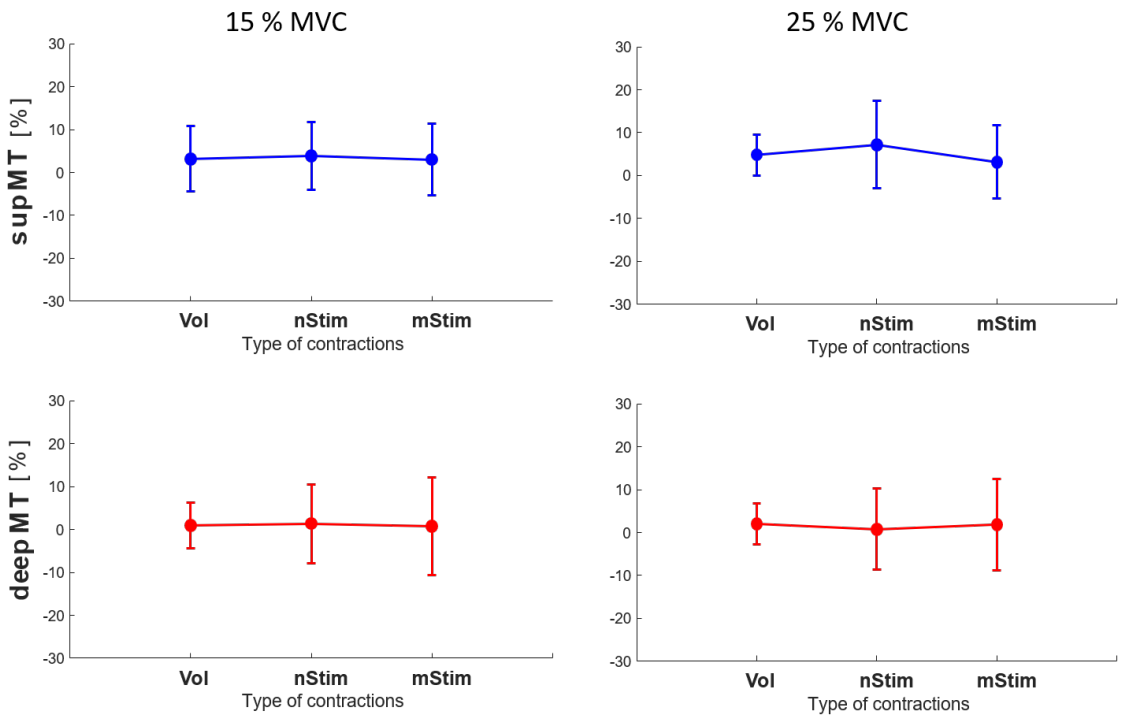

Figure 3.4: Mean and standard deviation between subjects for each contraction type of superficial (blue) and deep (red) MT percentage change with reference to the rest condition. None significant difference was found.

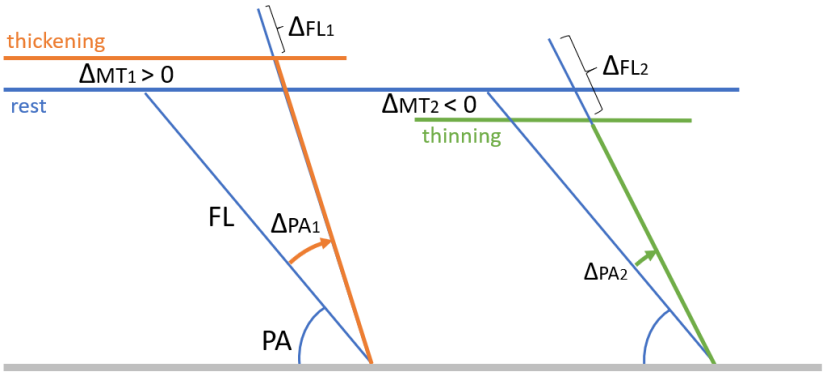

Figure 3.5: Scheme of effects of changing in FL and PA based on the model in paragraph 1.4.1 of TA. It is highlighted only 2 fascicles of one compartment with different conditions applied that lead to muscle thickening (1) or thinning (2).

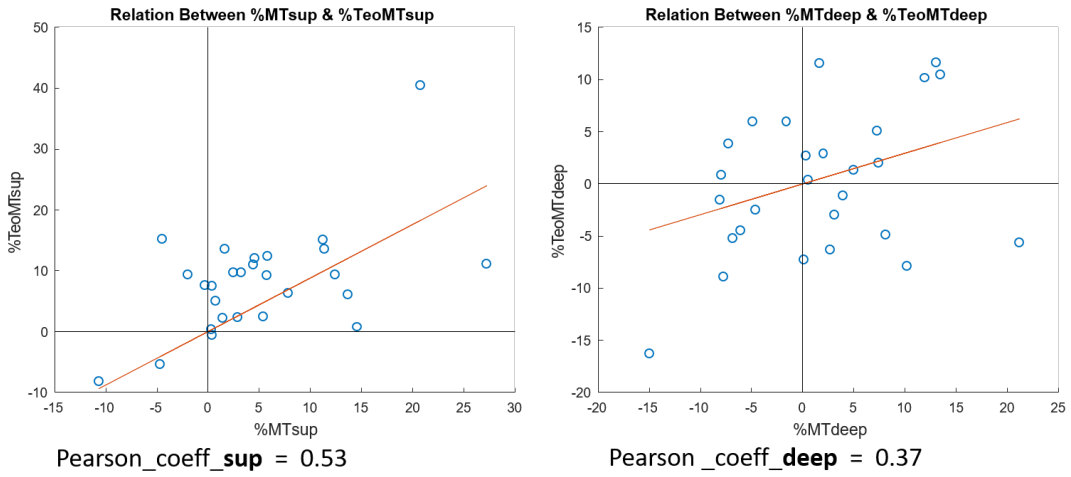

Figure 3.6: Correlations between MT calculated from $MT = FL{\cdot}\sin PA$ (theoretical) and MT manually evaluated from images (experimental), for both superficial and deep compartment.

As shown in Fig. 3.6, we found positive although and significant correlation between theoretical and experimental thickness (e.g. a theoretical thickening/thinning corresponds respectively to an experimental thickening/thinning). However, the correlation coefficient (i.e. Pearson) was not close 1 because evidently the used architectural model is not completely faithful to reality. Taking into account that thickening/thinning contributes simultaneously but differently for upper and deeper compartment, the effects of a contraction can not be clearly identified. Indeed the sum between superficial and deep changes may often be around zero or at least very low and then problematic to analyse as more affected by measurement errors. Therefore, separated evaluation of FL and PA is required to highlight differences among stimulation types.

3.4.2 Fascicle Length (FL)

Mean FL and the associated standard deviations are shown in Fig. 3.7. The percentage change in FL during Vol and nStim contractions did not show statistical significant differences for both MVC level for the superficial compartment. Instead, superficial FL in mStim considerably differs from the other two types, and in particular the percentage change was lower (i.e. more shortening) at both 15% and 20%. In the deep compartment, there was not any differences among contraction types at 15% of MVC. However, significant differences appeared at the higher percentage level. In particular, deep compartment in mStim differed from Vol and nStim (which are equal to each other), again in terms of greater FL shortening. This was contrary to our hypothesis, because we did not expect such a condition. However, our simplified model of TA architecture does not take into account possible passive movements of the fascicle. For instance, deep compartment fascicles during mStim might be dragged from the movements of central aponeurosis pulled by superficial fascicles strongly activated by such a stimulation. Indeed, the deep fascicle during mStim shortened more with reference to other contraction types because of this pulling of the superior compartment. Moreover, the assessment of FL is generally affected by the relative positions of the aponeurosis but as described in section 3.2 deep portions of TA often has not high definition, especially with regard to the deep aponeurosis.

3.4.3 Pennation Angle (PA)

The results of variable "PA" are shown in Fig. 3.8. At the lowest percentage of the MVC, no statistical differences have been observed. Instead, at 25% of MVC, the percentage change in superior PA in case of mStim contractions markedly differs from both Vol and nStim. Indeed, as hypothesized the superior compartment is preferentially activated (i.e. increasing in PA) during mStim with respect to the others contraction types. Although the initial hypothesis was that mStim may not activate the deep muscle portion, there was no significant differences in deep PA changing of such a contraction with both Vol and nStim indicating that this muscle

portion activates similarly in every condition. Moreover for what concerns the deep PA, time there was a difference also between Vol and nStim contractions. Specifically, nStim generated greater PA changing of for deep compartment. This may be based on the fact that superficial layers of TA contain a higher proportion of type I muscle fibers than deeper layers [72]. Indeed, nStim activates preferentially MUs of type II (because larger than type I and easily excitable) that are stronger and may generate more movement of those.

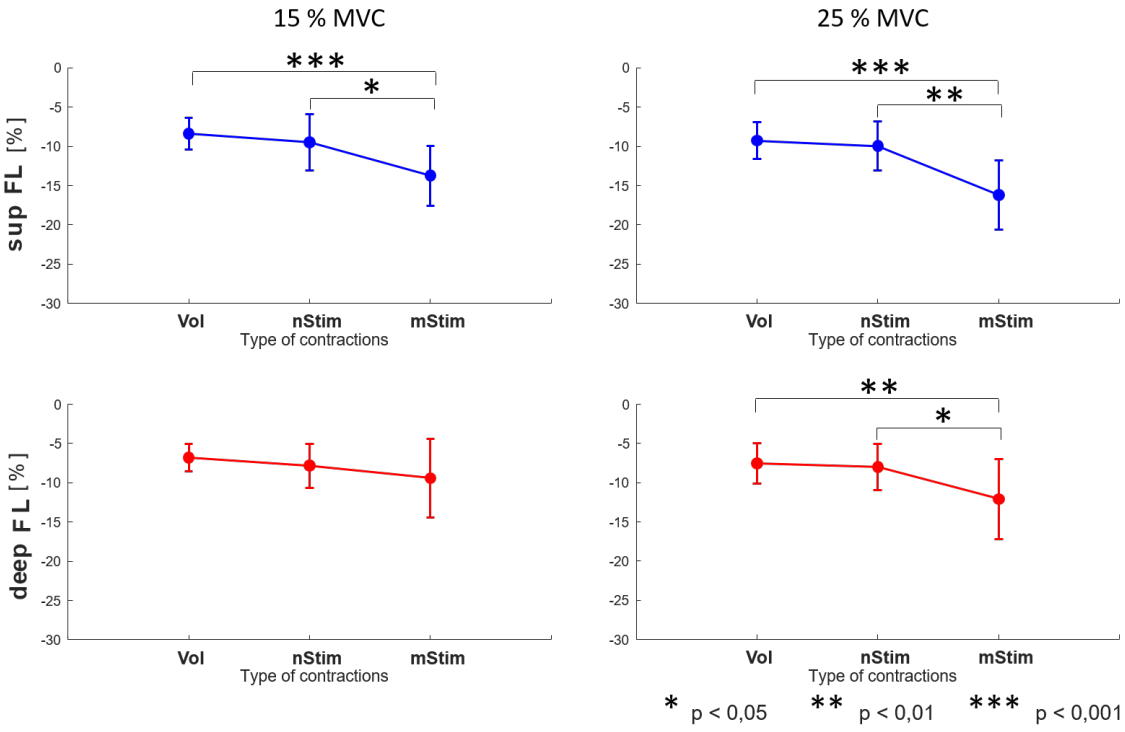

Figure 3.7: Mean and standard deviation between subjects for each contraction type of superficial (blue) and deep (red) FL percentage change with reference to the rest condition. Significant differences were found between mStim and nStim or Vol.

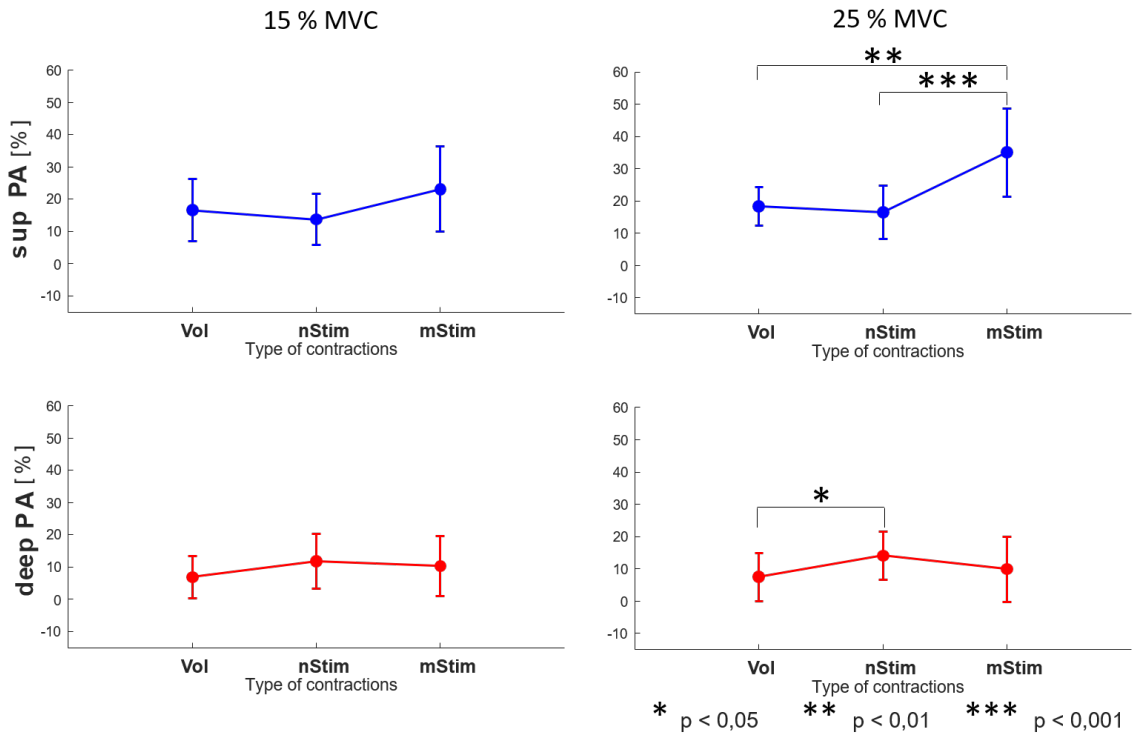

Figure 3.8: Mean and standard deviation between subjects for each contraction type of superficial (blue) and deep (red) PA percentage change with reference to the rest condition. Significant differences were found only at 25 % MVC.

3.5 Superficial vs Deep Analysis

In order to asses differences in architectural changes between superficial and deep portion of TA, repeated-measures variance analysis (ANOVA) was performed between their architectural parameters for both percentage level (Fig. 3.9 and 3.10). First of all, it is possible to notice that on average changes in the inferior compartment was less prominent for every contraction type, so the fascicle shortens and the PA rises to a smaller extent than in the superior compartment. However, these differences was statistically significant in mStim contractions indicating a relevant activation of superior muscle portion compared with the deep (as hypothesized). Therefore, comparing mStim at 25% of MVC with the 15%, the difference in PA increased but that in FL decreased, thus indicating that deeper fascicles may be

pulled by those in the superior portion. Physiological contractions (i.e. Vol) showed no differences in FL changing between the two portions, instead these appear in changing of PA but in smaller amount than in mStim. For what concerns nStim, the two muscle portions showed the same percentage changes for both FL and PA, thus indicating the same behaviour as Vol with regard to the fascicles shortening. Instead the PA changing shows almost equal activation between the upper and lower portions contrary to the general average (i.e. less activation of the deeper compartment).

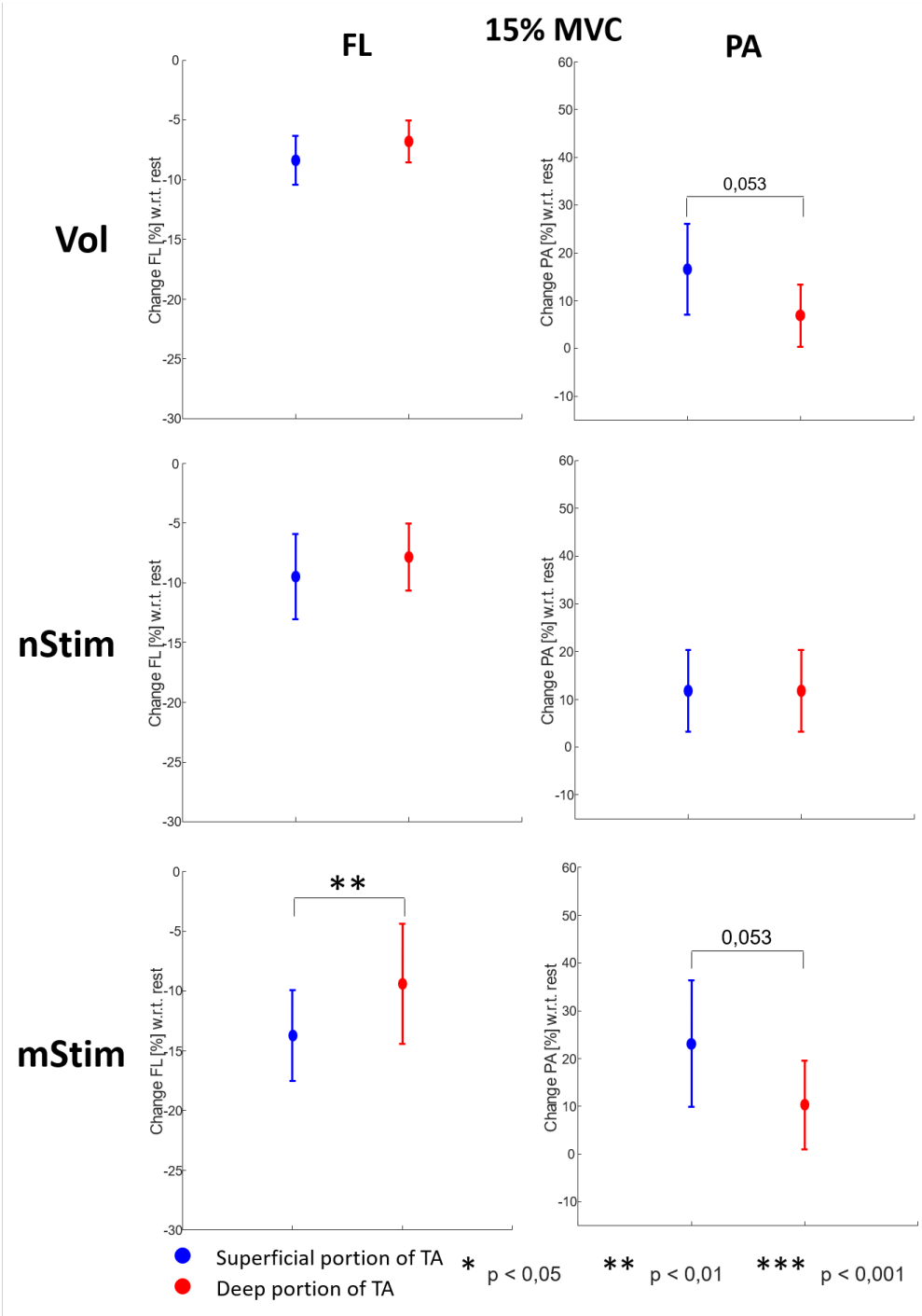

Figure 3.9: Comparison of FL (left column) and PA (right column) of superficial and deep muscle compartment for each contraction type at 15% of MVC.

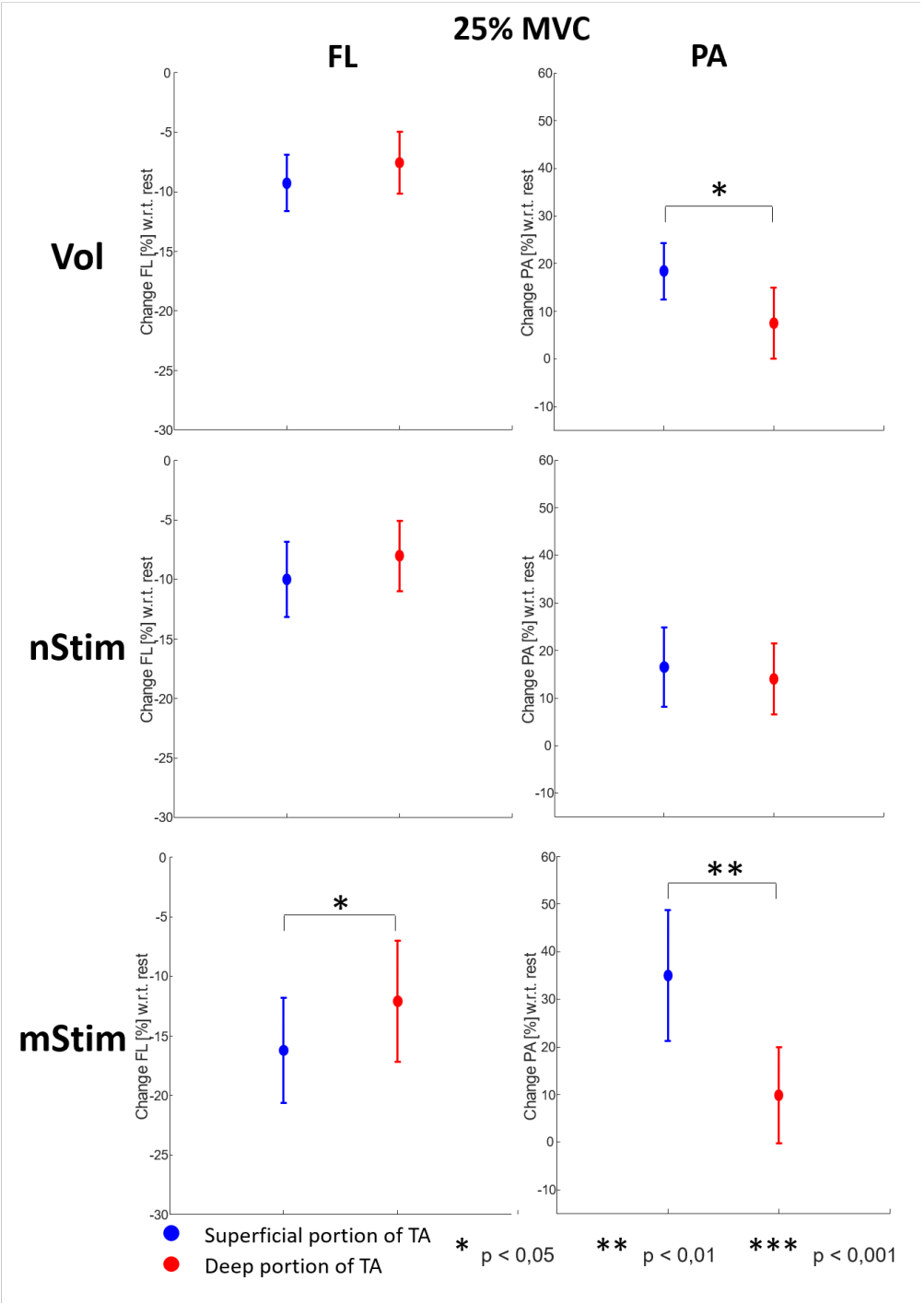

Figure 3.10: Comparison of FL (left column) and PA (right column) of superficial and deep muscle compartment for each contraction type at 25% of MVC.

3.6 Final discussion

The hypothesized behaviour was better observed for the contraction at 25% MVC which is probably associated to the fact that the degree of recruitment is higher. Therefore the output generated in terms of structural movements is more evident and differences among contraction types can be better observed. It should be noted that comparing the variables of interest for the same force output (like-with-like comparison) for different contraction types, clearly leads to differences in the architecture changing among them. Indeed, a specific level of voluntarily generated force is certainly produced by several MUs distributed in the muscle that CNS rotates and recruits over time (at a definitely lower frequency) in order to generate a fused and efficient contraction. Instead, during electrical-elicited contractions, activated MUs are less and always belonged to the same population, therefore the level of activation of these will have to be higher (in terms of firing rate) to get the same output. Finally, the architectural movements generated by such activations would be dissimilar at the same MVC level.

In Fig. 3.12 the results are represented in the Cartesian plane with the percentage change of FL in the x-axis and PA in the y-axis. This graph allows to compare the effects of different types of contraction (symbol coding) simultaneously on PA and FL and also to evaluate differences between compartments (colour coding). Noteworthy, mStim has a large effect on TA superficial portion (in terms of changing of FL and PA); additionally the lower compartment seems to be "pulled" along the x-axis (FL) as the level of force increases and not as much as along the y-axis (PA). This last evidence would once again suggests that passive movements may play an important role in such analysis. It may be considered that PA highlighted better differences among contraction types (probably due to better image definition) and also between superior and inferior compartment. In Vol contractions the percentage change in FL was similar between upper and lower portion, instead the PA was higher for the upper rather than the lower. Fig. 3.11 schematically represents the effects on TA architecture, specified above. The important point is that nStim is not different from Vol (except for a slight increase in the PA for the lower part). Instead, mStim differs greatly from nStim and Vol in the upper portion because PA

and FL increase, denoting a huge difference with the deep compartment in which fascicles seems to shorten without a correspondent PA increase (passive movement). Finally, a combination of these two stimulations could still provide advantages due to the fact that there may be an activation of a greater number of MUs divided between the upper and lower compartments, which therefore leads to a contraction much more similar to the physiological one.

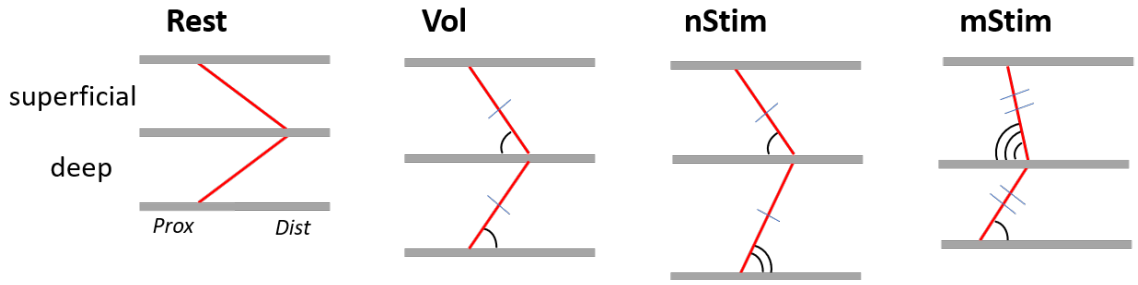

Figure 3.11: Schematic representation of architectural effects on TA. The three aponeurosis (grey) and a fascicle (red) per muscle portion (i.e. sup and deep) schematize the TA architecture. Blue rods on the fascicle indicate the activation degree (in terms of shortening) and black lines indicate the increasing degree of PA.

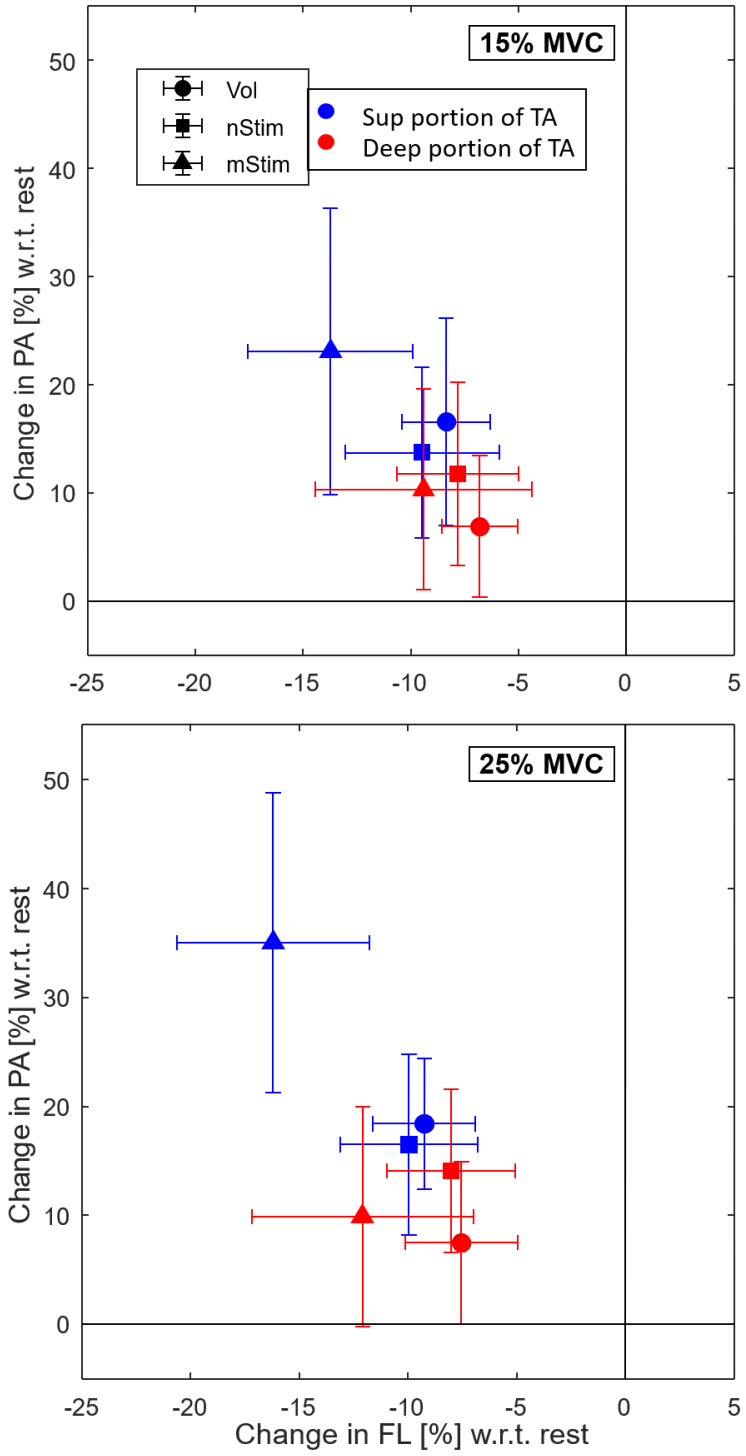

Figure 3.12: Cartesian representation of the means and standard deviations of percentage FL change (x-axis), and percentage PA change (y-axis) for both MVC levels.

Chapter 4

Proof of concept

4.1 Study objective

To further proof our concept, we wanted to test whether the novel method of stimulation introduced by Collins et al. (i.e. iNMES) would really result in less muscle fatigue than traditional methods. For this purpose a brief protocol for interleaved stimulation was designed. Finally, the muscle fatigue profiles were compared for three types of stimulation: muscle stimulation (mStim), nerve stimulation (nStim) and Interleaved stimulation (iStim). The first method (i.e. standard NMES) would produce contractions by repetitive recruitment of MUs that are located superficially in the TA muscle belly. Instead, nStim would produce contractions by repetitive recruitment of MUs that are distributed throughout the TA muscle belly. To determine whether there were differences in muscle fatigue, the mechanical output generated by TA (i.e. ankle dorsiflexion torque), should be registered along time while electrical stimulation is delivered through these electrode locations (muscle, nerve, both), so as to produce a fused contraction. We expected later occurrence of torque decline in our fatigue protocol (i.e., after more time) for iStim, because of the fact that more recruited MUs are also exchanged between pulses. Actually with the interleaved stimulation the frequency of a single site (either muscle or nerve) can be halved and the current intensity reduced, but even more MUs are recruited to produce the same output with less fatigue occurrence.

4.2 Materials and Methods

The experimental setup was simpler than that used to test the effect of stimulation on architectural features, indeed the designed fatigue protocol consists only in force registration during electrical-elicited contractions delivered in 3 modalities. This torque acquisition was made through the same setup exposed in the section 2.1.1 (i.e. isometric brace). Therefore, the same Graphical User Interface used in the main study (paragraph 2.1.5), was applied to register and display force traces. Also in this case, a constant-current neuromuscular stimulator, but that would allow the use of multiple output channels at the same time, was used. In particular, a RehaStim 8-channel stimulator (Hasomed Inc., Germany) (Fig. 4.1 A) was used to generate pulse trains transmitted via a set of transcutaneous disposable adhesive snap electrodes (the same as main study) placed over TA muscle belly and CP nerve trunk. In such a case, the wave form was necessarily biphasic (Fig. 4.1 B) with a fixed pause of 100 μs between the two phases of the pulse. For our purpose pulse width of 100 μs was selected. A script Matlab allowed to program the stimulator so as to separately modulate the current of two preselected channels during stimulation is running. The frequency can be also programmed starting the script.

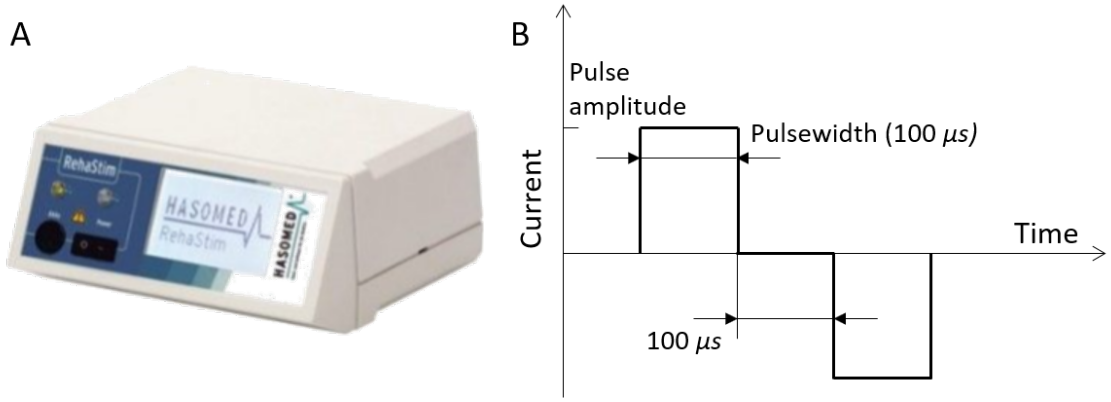

Figure 4.1: RehaStim programmable stimulation device (A) and definition of pulse width and current amplitude of biphasic wave form (B).

4.3 Protocol

One participant with no history of neurological or musculoskeletal impairment or disease was enrolled. We had to apply 3 different types of stimulation:

- **mStim**: electrodes positioned over the muscle belly (as in *Motor points identification* in section 2.1.2), frequency stimulation set to 40 pps.
- **nStim**: electrodes positioned in a way to stimulate CP (as in *Nerve course identification* in section 2.1.2), frequency stimulation set to 40 pps.
- **iStim**: electrodes positioned in both sites, with total stimulation frequency of 40 pps but exchanged between sites (thus 20 pps per site and 25 ms offset).

In case of iStim, we tried to achieve half of the output by the nerve and half by the muscle, hence we started rising the amplitude of the channel for nStim reaching the half of 25 % MVC, and then the same for mStim channel to reach the required level. The fatigue protocol consisted in the application of one of these stimulations to obtain force at 25 % of MVC, during time as long as the output force goes down 10 % of MVC, and then repeated equally for other stimulations. After each stimulation, a rest period of 10 minutes was ensured to completely relax the muscle and recover from fatigue. After all, 3 traces of registered force for each stimulation types can be analysed. The order of stimulation was: nStim, mStim and iStim.

4.4 Results

The subject terminated the experiment, reporting some discomfort (apart that associated with fatigue occurrence), in particular at the beginning of nStim that is reduced along the test but mainly during all mStim that increase along the test. During iStim the perception of discomfort was smaller, only at the end it increase a bit in the muscle region between electrodes over the belly. For the nStim elicited contraction was used a current amplitude of 20 mA, while for mStim was used 54 mA and finally during iStim, the amplitude for nerve channel was 18 mA and for muscle was 28 mA.

4.4.1 Qualitative torque-time analysis

As shown in Fig. 4.2, in which the torque normalized by the value of MVC is represented along the time, there is no relevant difference in mechanical fatigue onset between mStim and nStim. The stimulation ended after 190 seconds in nStim and after 220 sec in mStim because 10 % of MVC was reached. For iStim, the stimulation was interrupted after 310 s neither reached 15 % of MVC. Considering that TA muscle contains mostly fibers of type I (i.e. small, slow, fatigue-resistant) because it is involved on maintaining upright posture and is crucial for gait, the fatigue onset is belated. However, less muscle fatigue was detected during mStim than nStim. The main explanation of this can be found in the fact that nStim would principally elicit type II fibers (because larger than type I and easily excitable) that are less fatigue resistant. Instead, the recruitment of mStim depends from the geometry and position of MU branches under the stimulation electrodes. We mentioned that iStim would recruit mainly distinct MU pools with exchanged pulses (between nerve and muscle), and also discharge frequency of MUs would be of 20 Hz compared with the 40-Hz discharge frequency of MUs recruited during mStim and nStim. All this results in less neuromuscular propagation failure (less high-frequency fatigue) and less overall muscle fatigue as shown also here by the torque output.

Further analysing the descendent phase of the torque, i.e. the phase where the electrical stimulation is stable starting from the maximum level, the linear interpolation of each type of contraction was calculated with slope and y-axis intercept were completed (Fig. 4.2 below). We defined the failure time as the period in which the torque level declined of 50% with reference to the initial value. In this way differences of stimulation effects may be quantitatively compared. For what concerns iStim, there was a much slower decrease (i.e. lowest slope) and an y-axis intercept close to 100% of the starting value which precisely indicates that the torque declined in a more linear manner. Indeed, iStim doubled its failure time with respect to mStim and nStim because of its low slope value. nStim and mStim had comparable failure times (about 170 and 160 seconds respectively) and slopes (0.33 %/s and 0.28 %/s respectively). nStim had the highest y-axis intercept because initially the torque slowly declined and then suddenly drop after a while, indeed the its slope

value was the smallest one. Instead, during mStim the torque declined faster at the beginning (smaller intercept with y-axis) and then stabilized and decreased more gradually. Then its slope value resulted higher than the nStim value. The slope of the lines indicated the degree of percentage loss of torque over time, which on the other hand was greater for nStim compared to mStim. This once again indicates that nStim was less fatigue resistant because it elicit preferentially type II fibers. The use of iStim for instance has the potential to extend both walking time and distance if implemented in foot drop stimulators.

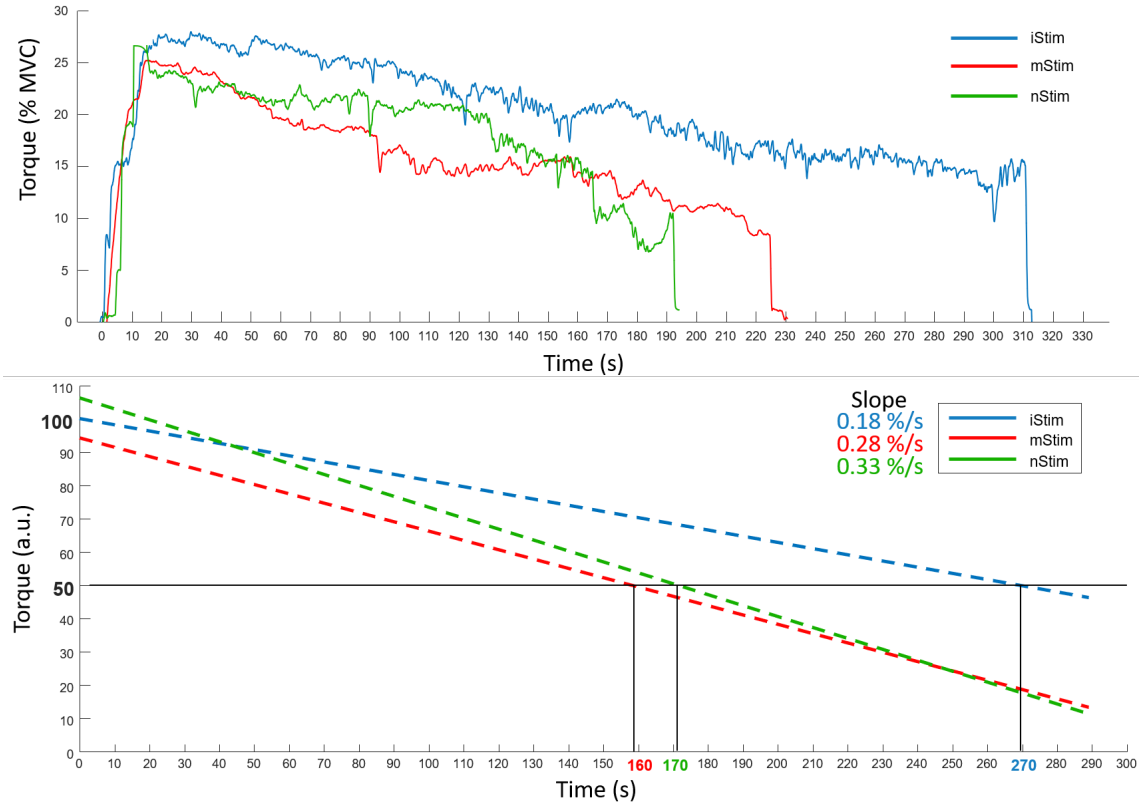

Figure 4.2: Above: torque traces during fatigue protocol normalized with reference to MVC for each stimulation type. Below: linear regressions of descending torque phases normalized to the starting value of each stimulation type; slopes (%/s) of linear regression are presented and the time when the torque decline by 50 % with respect to the initial value.

Chapter 5

Conclusion

It is well known that muscle contractions generated by electrical stimulations are associated with rapid development of neuromuscular fatigue. To reduce the issue of fatigability in electrically-elicited contractions, several types of stimulation have been developed. Different approaches were sought to to reduce the overall Motor Unit (MU) discharge rates and increase spatial MU recruitment (e.g. distributed and sequential stimulation), but also to achieve a more physiological MU recruitment order relying on reflex pathways (e.g. afferent stimulation).

Among the methods for fatigue reduction, Interleaved stimulation (iStim) is a recent approach in which electrical stimuli are intermittently provided to muscle and nerve sites to stimulate different populations of MU. The extent to which fatigue is reduced with iStim depends on the degree of overlap between the populations of MUs activated by the two stimulations (i.e. mStim and nStim). In general, groups of MUs activated by either mStim or nStim are different because of the different MU recruitment order of nStim and mStim (i.e. inverse vs random). Geometric factors may also play a relevant role in this differentiation, indeed superficial MUs (those closest to the stimulating electrodes) are recruited preferentially during stimulation over a muscle belly (mStim), whereas for stimulation over the CP nerve trunk (nStim), it was found that recruited MUs were randomly distributed evenly throughout the muscle regardless of stimulation amplitude.

In this study we investigated whether and to which degree the stimulation site (mStim or nStim) affected the architectural changes in the superficial and deep TA compartments. For this reason, Ultrasound (US) imaging was used to quantify muscle tissue displacement associated with MU activations by measuring morphometric parameters, such as Muscle Thickness (MT), Fascicle Length (FL) and Pennation Angle (PA) during contractions evoked by nStim, mStim and voluntarily performed. It was found that architectural changes in nStim contractions were similar to those observed in voluntary contraction (i.e. the PA and FL of the superficial and deep muscle portions changed similarly). Instead, mStim contractions led to a relevant activation (and architectural changes) of the upper compartment compared with the deeper one.. These findings suggest that in TA interleaved stimulation can be used to activate different muscle portions, with possible implications for the reduction of electrically-induced fatigue. Indeed, by interleaving the recruitment of different MUs either located superficially (during mStim) or distributed throughout the muscle (during nStim), this type of stimulation allows to obtain the required force output with a low-frequency activation of different MU populations.

As demonstrated in the Proof of Concept, iStim doubled the time to task failure with respect to mStim and nStim because of its lowest rate of force reduction. We demonstrated the fatigue resistance capability of iStim in the worst case, i.e. sustained contraction, indeed in FES applications, the activations are intermittent. Although we demonstrated that the fatigue has been reduced, a number of considerations must be taken into account for future perspectives of this technique in applied scenarios. For instance, the robustness of nerve stimulation must be verified in terms of problems resulting from the selectivity of the elicited contractions (e.g. dorsiflexion vs eversion in CP nerve stimulation). Indeed, usage of iStim may not be replicable in dynamic conditions due to a shift of the nerve stimulation point. Therefore, an implantable foot drop stimulator with a cuff electrode around the nerve (which allows selective stimulation) may be modified with the addition of interleaved muscle stimulation. This would complicate the setup (at least two more surface electrodes) and the control of the stimulation (pulses must be delivered intermittently to stimulation sites), but on the other hand would provide the potential

to extend both walking time and distance. Besides FES applications in which the main aim is related to fatigue reduction, the larger portion of MU spectrum activated by different stimulation sites, demonstrated in this study, suggests a possible applications in rehabilitation to preserve or recover muscle mass more efficiently.

Bibliography

[1] E Hultman, H Sjöholm, I Jäderholm-Ek, and J Krynicki, "Evaluation of methods for electrical stimulation of human skeletal muscle in situ", *Pflügers Archiv*, vol. 398, no. 2, pp. 139–141, 1983, ISSN: 1432-2013.

[2] R. M. A. Rainoldi, M.A. Minetto, *Biomedical engineering in exercise and sports*. Torino: Minerva Medica, 2006, ISBN: 978-88-7711-530-0.

[3] A. Botter, *Investigation of the neuromuscular system during involuntary muscle contractions. Methodological issues and clinical applications [Risorsa elettronica] / Alberto Botter ; rel. Roberto Merletti*, Torino, 2011.

[4] M. H. Trimble and R. M. Enoka, "Mechanisms Underlying the Training Effects Associated with Neuromuscular Electrical Stimulation", *Physical Therapy*, vol. 71, no. 4, pp. 273–280, 1991.

[5] G. K. Fitzgerald and A Delitto, "Neuromuscular electrical stimualtion for muscle strength training", *Biomedical engineering in exercise and sports. Edizioni Minerva Medica, Torino*, pp. 199–207, 2006.

[6] J. N. Gibson, W. L. Morrison, C. M. Scrimgeour, K. Smith, P. J. Stoward, and M. J. Rennie, "Effects of therapeutic percutaneous electrical stimulation of atrophic human quadriceps on muscle composition, protein synthesis and contractile properties", *European Journal of Clinical Investigation*, 1989, ISSN: 13652362.

[7] N. A. Maffiuletti, "Physiological and methodological considerations for the use of neuromuscular electrical stimulation", *European journal of applied physiology*, vol. 110, no. 2, pp. 223–234, 2010.

[8] B. M. Doucet, A. Lam, and L. Griffin, "Neuromuscular electrical stimulation for skeletal muscle function", *The Yale journal of biology and medicine*, vol. 85, no. 2, p. 201, 2012.

[9] J. H. Moe and H. W. Post, "Functional electrical stimulation for ambulation in hemiplegia.", *The Journal-lancet*, vol. 82, pp. 285–288, 1962.

[10] D. B. Popović, "Advances in functional electrical stimulation (FES)", *Journal of Electromyography and Kinesiology*, vol. 24, no. 6, pp. 795–802, 2014.

[11] H. M. Franken, P. Veltink, and H. K. Boom, "Restoring gait in paraplegics by functional electrical stimulation", *IEEE Engineering in Medicine and Biology Magazine*, vol. 13, pp. 564–570, 1994.

[12] W. T. Liberson, "Functional electrotherapy: stimulation of the peroneal nerve synchronized with the swing phase of the gait of hemiplegic patients", *Arch Phys Med*, vol. 42, pp. 101–105, 1961.

[13] J. J. Laskin, E. A. Ashley, L. M. Olenik, and R. B. F. C, "Electrical stimulation-assisted rowing exercise in spinal cord injured people . A pilot study", vol. 31, pp. 534–541, 1993.

[14] M. Kjaer, "Why exercise in paraplegia?", *British Journal of Sports Medicine*, vol. 34, no. 5, pp. 322–323, 2000, ISSN: 0306-3674.

[15] D Dumitru, *Electrodiagnostic Medicine*. Hanley & Belfus, 1995, ISBN: 9781560530718.

[16] R. Merletti and D. Farina, *Surface Electromyography: Physiology, Engineering and Applications*. 2016, ISBN: 9781119082934.

[17] A. Botter, G. Oprandi, F. Lanfranco, S. Allasia, N. A. Maffiuletti, and M. A. Minetto, "Atlas of the muscle motor points for the lower limb: Implications for electrical stimulation procedures and electrode positioning", *European Journal of Applied Physiology*, vol. 111, no. 10, pp. 2461–2471, 2011, ISSN: 14396319.

[18] F. H. Netter, *Netter. Atlante anatomia umana. Selezione tavole per Scienze motorie e fisioterapia*. Edra, 2015, ISBN: 9788821440168.

[19] A. Botter and R. Merletti, "EMG of electrically stimulated muscles", in *Surface Electromyography: Physiology, Engineering and Applications*, 2016, ISBN: 9781119082934.

[20] E. P. Zehr, *Considerations for use of the Hoffmann reflex in exercise studies*, 2002.

[21] A. Botter and T. M. Vieira, "Optimization of surface electrodes location for H-reflex recordings in soleus muscle", *Journal of Electromyography and Kinesiology*, 2017, ISSN: 18735711.

[22] E. Pierrot-Deseilligny and D. Burke, *The Circuitry of the Human Spinal Cord*. 2012, ISBN: 9781139026727.

[23] A. J. Bergquist, J. M. Clair, O Lagerquist, C. S. Mang, Y Okuma, and D. F. Collins, "Neuromuscular electrical stimulation: implications of the electrically evoked sensory volley", *European journal of applied physiology*, vol. 111, no. 10, p. 2409, 2011.

[24] D. F. Collins, D Burke, and S. C. Gandevia, "Large involuntary forces consistent with plateau-like behavior of human motoneurons.", *The Journal of neuroscience : the official journal of the Society for Neuroscience*, 2001, ISSN: 1529-2401.

[25] R. Merletti, A. Botter, F. Lanfranco, and M. A. Minetto, "Spinal Involvement and Muscle Cramps in Electrically Elicited Muscle Contractions", *Artificial Organs*, 2011, ISSN: 0160564X.

[26] N. A. Maffiuletti, M. Pensini, G. Scaglioni, A. Ferri, Y. Ballay, and A. Martin, "Effect of electromyostimulation training on soleus and gastrocnemii H- and T-reflex properties", *European Journal of Applied Physiology*, vol. 90, no. 5-6, pp. 601–607, 2003, ISSN: 14396319.

[27] R. Merletti, M. Knaflitz, and C. DeLuca, "Electrically evoked myoelectric signals.", *Critical reviews in biomedical engineering*, vol. 19 4, pp. 293–340, 1992.

[28] A. Delitto, M. J. Strube, A. D. Shulman, and S. D. Minor, "A Study of Discomfort with Electrical Stimulation", *Physical Therapy*, 2017, ISSN: 0031-9023.

[29] B. Doucet, A Lam, and L Griffin, "Neuromuscular Electrical Stimulation for Muscle Rehabilitation", *Yale Journal of Biology and Medicine*, vol. 85, pp. 201–215, 2012, ISSN: 1551-4056; 0044-0086.

[30] M. Vanderthommen, J. C. Depresseux, L. Dauchat, C. Degueldre, J. L. Croisier, and J. M. Crielaard, "Spatial distribution of blood flow in electrically stimulated human muscle: A positron emission tomography study", *Muscle and Nerve*, 2000, ISSN: 0148639X.

[31] G. R. Adams, R. T. Harris, D. Woodard, and G. A. Dudley, "Mapping of electrical muscle stimulation using MRI", *Journal of Applied Physiology*, 2017, ISSN: 8750-7587.

[32] R. M. Enoka, "Activation order of motor axons in electrically evoked contractions", *Muscle and Nerve*, 2002, ISSN: 0148639X.

[33] E. Henneman, "Functional organization of motoneuron pools: the size-principle", *Integration in the nervous system*, pp. 13–25, 1979.

[34] J. A. Stephens and T. P. Usherwood, "The mechanical properties of human motor units with special reference to their fatiguability and recruitment threshold", *Brain research*, vol. 125, no. 1, pp. 91–97, 1977.

[35] M. Knaflitz, R. Merletti, and C. J. De Luca, "Inference of motor unit recruitment order in voluntary and electrically elicited contractions", *Journal of Applied Physiology*, 2017, ISSN: 8750-7587.

[36] C. M. Gregory and C. S. Bickel, "Recruitment Patterns in Human Skeletal Muscle During Electrical", *Journal of the american physical therapy association*, 2005, ISSN: 0031-9023.

[37] M. Jubeau, J. Gondin, A. Martin, A. Sartorio, and N. A. Maffiuletti, "Random motor unit activation by electrostimulation", *International Journal of Sports Medicine*, 2007, ISSN: 01724622.

[38] N. M. Malesevic, L. Z. Popovic, L. Schwirtlich, and D. B. Popovi, "Distributed low-frequency functional electrical stimulation delays muscle fatigue compared to conventional stimulation", *Muscle and Nerve*, vol. 42, no. 4, pp. 556–562, 2010, ISSN: 10974598.

[39] D Morgan, Y Huang, A Wise, U Proske, and I. E. Brown, "Distribution Stimulation of Skeletal Muscle", 1999.

[40] L. Z. Popović and N. M. Malešević, "Muscle fatigue of quadriceps in paraplegics: Comparison between single vs. multi-pad electrode surface stimulation", *Proceedings of the 31st Annual International Conference of the IEEE Engineering in Medicine and Biology Society: Engineering the Future of Biomedicine, EMBC 2009*, pp. 6785–6788, 2009, ISSN: 1557-170X.

[41] L. Z. P. Maneski, N. M. Malešević, A. M. Savić, T. Keller, and D. B. Popović, "Surface-distributed low-frequency asynchronous stimulation delays fatigue of stimulated muscles", *Muscle & Nerve*, vol. 48, no. 6, pp. 930–937, 2013, ISSN: 0148639X.

[42] A. J. Buckmire, D. R. Lockwood, C. J. Doane, and A. J. Fuglevand, "Distributed stimulation increases force elicited with functional electrical stimulation", *Journal of Neural Engineering*, vol. 15, no. 2, aa9820, 2018, ISSN: 17412552.

[43] D. G. Sayenko, M. R. Popovic, and K. Masani, "Spatially distributed sequential stimulation reduces muscle fatigue during neuromuscular electrical stimulation", *Proceedings of the Annual International Conference of the IEEE Engineering in Medicine and Biology Society, EMBS*, no. 4, pp. 3614–3617, 2013, ISSN: 1557170X.

[44] A. J. Bergquist, V. Babbar, S. Ali, M. R. Popovic, and K. Masani, "Fatigue reduction during aggregated and distributed sequential stimulation", *Muscle and Nerve*, vol. 56, no. 2, pp. 271–281, 2017, ISSN: 10974598.

[45] R Ruslee, J Miller, and H Gollee, "Investigation of Different Stimulation Patterns with Doublet Pulses to Reduce Muscle Fatigue", *21th IFESS Annual Conference*, vol. 10, no. 7, pp. 364–367, 2017.

[46] J. Dideriksen, K. Leerskov, M. Czyzewska, and R. Rasmussen, "Relation between the frequency of short-pulse electrical stimulation of afferent nerve fibers and evoked muscle force", *IEEE Transactions on Biomedical Engineering*, vol. 64, no. 11, pp. 2737–2745, 2017, ISSN: 15582531.

[47] A. J. Bergquist, M. J. Wiest, Y. Okuma, and D. F. Collins, "H-reflexes reduce fatigue of evoked contractions after spinal cord injury", *Muscle and Nerve*, vol. 50, no. 2, pp. 224–234, 2014, ISSN: 10974598.

[48] J. L. Dideriksen, S. Muceli, S. Dosen, C. M. Laine, and D. Farina, "Physiological recruitment of motor units by high-frequency electrical stimulation of afferent pathways", *Journal of Applied Physiology*, vol. 118, no. 3, pp. 365–376, 2015, ISSN: 8750-7587.

[49] D. C. James, M. C. Solan, and K. N. Mileva, "Wide-pulse, high-frequency, low-intensity neuromuscular electrical stimulation has potential for targeted strengthening of an intrinsic foot muscle: A feasibility study", *Journal of Foot and Ankle Research*, vol. 11, no. 1, pp. 1–10, 2018, ISSN: 17571146.

[50] S. Regina Dias Da Silva, D. Neyroud, N. A. Maffiuletti, J. Gondin, and N. Place, "Twitch potentiation induced by two different modalities of neuromuscular electrical stimulation: Implications for motor unit recruitment", *Muscle and Nerve*, vol. 51, no. 3, pp. 412–418, 2015, ISSN: 10974598.

[51] J. C. Dean, J. M. Clair-Auger, O. Lagerquist, and D. F. Collins, "Asynchronous recruitment of low-threshold motor units during repetitive, low-current stimulation of the human tibial nerve", *Frontiers in Human Neuroscience*, vol. 8, no. December, pp. 1–12, 2014, ISSN: 1662-5161.

[52] J. Duclay, "Evoked H-Reflex and V-Wave Responses During Maximal Isometric, Concentric, and Eccentric Muscle Contraction", *Journal of Neurophysiology*, vol. 94, no. 5, pp. 3555–3562, 2005, ISSN: 0022-3077.

[53] J. W. Lou, A. J. Bergquist, A. Aldayel, J. Czitron, and D. F. Collins, "Interleaved neuromuscular electrical stimulation reduces muscle fatigue", *Muscle and Nerve*, vol. 55, no. 2, pp. 179–189, 2017, ISSN: 10974598.

[54] A. J. Bergquist, M. J. Wiest, Y. Okuma, and D. F. Collins, "Interleaved neuromuscular electrical stimulation after spinal cord injury", *Muscle and Nerve*, vol. 56, no. 5, pp. 989–993, 2017, ISSN: 10974598.

[55] M. J. Wiest, A. J. Bergquist, and D. F. Collins, "Torque, Current, and Discomfort During 3 Types of Neuromuscular Electrical Stimulation of Tibialis Anterior", vol. 98, no. 9, pp. 779–785, 2018.

[56] L. Mesin, E. Merlo, R. Merletti, and C. Orizio, "Investigation of motor unit recruitment during stimulated contractions of tibialis anterior muscle", *Journal of Electromyography and Kinesiology*, vol. 20, no. 4, pp. 580–589, 2010, ISSN: 10506411.

[57] M. J. Wiest, A. J. Bergquist, H. L. Schimidt, K. E. Jones, and D. F. Collins, "Interleaved neuromuscular electrical stimulation: Motor unit recruitment overlap", *Muscle and Nerve*, vol. 55, no. 4, pp. 490–499, 2017, ISSN: 10974598.

[58] D. Coglianese, "Muscles: Testing and Function With Posture and Pain, ed 5 (with Primal Anatomy CD-ROM)", *Physical Therapy*, vol. 86, no. 2, pp. 304–305, 2006, ISSN: 0031-9023.

[59] J. C. Lee and J. C. Healy, "CHAPTER 60 - Sonography of muscle injury", in *Clinical Ultrasound (Third Edition)*, P. L. Allan, G. M. Baxter, and M. J. Weston, Eds., Third Edit, Edinburgh: Churchill Livingstone, 2011, pp. 1137–1157, ISBN: 978-0-7020-3131-1.

[60] I. Beggs, "CHAPTER 51 - Muscular ultrasound – introduction", in *Clinical Ultrasound (Third Edition)*, P. L. Allan, G. M. Baxter, and M. J. Weston, Eds., Third Edit, Edinburgh: Churchill Livingstone, 2011, pp. 1025–1029, ISBN: 978-0-7020-3131-1.

[61] Y. Okuma, A. J. Bergquist, D. F. Collins, M. Hong, and K. M. Chan, "Electrical stimulation site influences the spatial distribution of motor units recruited in tibialis anterior", *Clinical Neurophysiology*, vol. 124, no. 11, pp. 2257–2263, 2013, ISSN: 13882457.

[62] T. M. Vieira, M. C. Bisi, R. Stagni, and A. Botter, "Changes in tibialis anterior architecture affect the amplitude of surface electromyograms", *Journal of NeuroEngineering and Rehabilitation*, 2017, ISSN: 17430003.

[63] K. Sasaki, S. Toyama, and N. Ishii, "Length-force characteristics of in vivo human muscle reflected by supersonic shear imaging", *Journal of Applied Physiology*, vol. 117, no. 2, pp. 153–162, 2014, ISSN: 8750-7587.

[64] A. Moraux, A. Canal, G. Ollivier, I. Ledoux, V. Doppler, C. Payan, and J. Y. Hogrel, "Ankle dorsi- and plantar-flexion torques measured by dynamometry in healthy subjects from 5 to 80 years", *BMC Musculoskeletal Disorders*, vol. 14, 2013, ISSN: 1471-2474.

[65] I. D. Loram, E. F. Hodson-Tole, A. Botter, R. Merletti, and T. M. M. Vieira, "A novel system of electrodes transparent to ultrasound for simultaneous detection of myoelectric activity and B-mode ultrasound images of skeletal muscles", *Journal of Applied Physiology*, 2013, ISSN: 8750-7587.

[66] M. Barbero, R. Merletti, and A. Rainoldi, *Atlas of Muscle Innervation Zones*. 2012, ISBN: 978-88-470-2462-5.

[67] C. J. De Luca and R. Merletti, "Surface myoelectric signal cross-talk among muscles of the leg", *Electroencephalography and Clinical Neurophysiology*, 1988, ISSN: 00134694.

[68] D. J. Farris and G. A. Lichtwark, "UltraTrack: Software for semi-automated tracking of muscle fascicles in sequences of B-mode ultrasound images", *Computer Methods and Programs in Biomedicine*, vol. 128, pp. 111–118, 2016, ISSN: 18727565.

[69] N. J. Cronin, C. P. Carty, R. S. Barrett, and G. Lichtwark, "Automatic tracking of medial gastrocnemius fascicle length during human locomotion", *Journal of Applied Physiology*, vol. 111, no. 5, pp. 1491–1496, 2011, ISSN: 8750-7587.

[70] J. G. Gillett, R. S. Barrett, and G. A. Lichtwark, "Reliability and accuracy of an automated tracking algorithm to measure controlled passive and active

muscle fascicle length changes from ultrasound", *Computer Methods in Biomechanics and Biomedical Engineering*, vol. 16, no. 6, pp. 678–687, 2013, ISSN: 14768259.

[71] B. D. Lucas, T. Kanade, and Others, "An iterative image registration technique with an application to stereo vision", 1981.

[72] K. B. Henriksson-Larsén, J. Lexell, and M. Sjöström, "Distribution of different fibre types in human skeletal muscles. I. Method for the preparation and analysis of cross-sections of whole tibialis anterior", *The Histochemical Journal*, 1983, ISSN: 00182214.